POSSIBLE CHAOTICITY IN CONDENSED MATTER SYSTEM

by

Orhan Özgür Aybar

B.S., Physics, Boğaziçi University, 2006

Submitted to the Institute for Graduate Studies in
Science and Engineering in partial fulfillment of
the requirements for the degree of
Master of Science

Graduate Program in Physics

Boğaziçi University

2008

POSSIBLE CHAOTICITY IN CONDENSED MATTER SYSTEM

APPROVED BY:

Prof. Yani Skarlatos .....
(Thesis Supervisor)

Prof. Avadis Simon Hacınlıyan.....
(Thesis Co-supervisor)

Prof.Haluk Beker .....

Prof. Naci İnci .....

Assist. Prof. Gökhan Şahin .....

DATE OF APPROVAL: 06.08.2008

ACKNOWLEDGEMENTS

I owe special thanks to my supervisor Prof. Dr. Yani Skarlatos for his understanding, never ending support, his calmness and critical advice. He was always ready to discuss on the issues of this work.

I would like to express my gratitude to my co-supervisor Prof. Dr. Avadis Simon Hacınlıyan for his never ending patience in directing me throughout my M. Sc. Studies, teaching me a great deal, helping and motivating me in every way to become a good scientist. He always gave special attention to the work load I was given so that I could finish this study on time. Despite the fact that it is hard to work with a person of applied physics background, he accepted me to his research group without any doubts. Whenever I need help, I know that he is always willing and ready.

I would like to give my regards to Prof. Dr. Haluk Beker and Prof. Dr. Naci İnci for their critical reading and helpful suggestions. I also would like to thank to Prof. Dr. Haluk Beker for the EMT Course. It was a long story; I will never forget how the course improved me.

I would like to thank the members of our research group, especially "Big Brother" Assist. Prof. Dr. Gökhan Şahin and "Brother" Kaan Atak, for their friendship, cooperation, support, for their critical advice and relaxing attitude during the progress of my work.

I would like to thank Prof. Dr. Ayşe Erzan; first for mentioning the embedding dimension concept during my presentation in the Statistical Physics Days, IFG, and then for her advice during the preparation of this work.

I would also like to thank to my dean Prof. Dr. Ömer Gökay, the Faculty of Commerce and my colleagues in the Department of Information Systems and Technologies for their understanding and strong support.

I would like to thank to Dr. Özgül Kurtuluş for the data sets that were taken in the Boğaziçi University Solid State Laboratory.

My grateful thanks are due to my affectionate parents, Hülya and Erol Aybar for their patience and never ending support. They have never withheld their support and understanding during the hard task of writing a M.S. Thesis. Without them life would be unbearable. Whenever I lost my hope and concentration, they were always ready. They were the tower of strength thanks to which I was able to recover my motivation and concentration. This thesis is dedicated to my family to whom I owe everything.

ABSTRACT

POSSIBLE CHAOTICITY IN CONDENSED MATTER SYSTEM

Thin films of polymers are expected to have irregular transient current characteristics under constant voltage. In polymers with water absorbing property such as Polyethylene Glycol, the irregularity also depends on the relative humidity. This study is aimed at studying this irregular current as a function of slowly varying relative humidity.

The time dependence of the relative humidity was adequately modelled by stretched exponential absorption model. Time series analysis and detrended fluctuation analysis were applied both to the entire data and binned data according to both time and relative humidity intervals and instances of chaotic behavior were observed.

ÖZET

YOĞUN MADDE SİSTEMLERİNDE OLASI KAOTİK DAVRANIŞ

İnce polimer filmlerin sabit gerilim altında zamanda düzensiz geçici akım davranış gösterdiği bilinmektedir. Polietilen glikol örneğindeki gibi suyu emme özelliği olan polimerlerdeki akım düzensizliği göreli neme de bağlı olacaktır. Bu çalışmanın amacı düzensiz akımı zaman içinde yavaş değişen göreli nemin fonksiyonu olarak incelemektir.

Nemin zamana bağlılığı gerilmiş üstel soğrulma modeli ile modellenmiştir. Zaman serisi analizi ve eğilimsizleştirilmiş dalgalanma analizi tüm veri takımına, zaman aralığı dilimlerine ayrılmış ve göreli nem aralığı dilimlerine ayrılmış veri takımlarına ayrı ayrı uygulanmıştır. Olası kaotik davranışlar gözlemlenmiştir.

TABLE OF CONTENTS

LIST OF FIGURES

LIST OF SYMBOLS/ABBREVIATIONS

$A(t)$	Autocorrelation function
$F(n)$	Root mean square fluctuation
$I(X;Y)$	Mutual information
m	Embedding dimension
n	Topological dimension
$P_{XY}(x_i;y_j)$	Joint probability of x_i and y_j
R_m	Euclidean distance
$S(\Delta n)$	Stretching factor
$S(t)$	One dimensional signal
$S(x_i)$	Time evolution of dynamical observable
t	Delay time
$U(s_{n_0})$	Neighborhood of s_{n_0}
x_i	Dynamical system
$y(k)$	Integrated time series
ϵ	Neighborhood size
DFA	Detrended fluctuation analysis
FFT	Fast fourier transform
PAF	Perfluoroalkylethylalcohol
PEG	Poly Etilen Glikol
PEGH	Hydrogenated Poly Ethylene Glycol

1. INTRODUCTION

The aim of this thesis is to study irregular transient current through thin films made of polymers. Such polymers are known to have irregular current characteristics under constant voltage and varying relative humidity. In this study the current through a thin film of Gamma-isocyanatopropyltriethoxysilane added Polyethylene glycol (PEG-Si) as a function of increasing relative humidity at equal time steps is analyzed for chaoticity. The data that we analyzed were taken by a computerized data acquisition system while the relative humidity was increased and the current was measured at uniform time intervals. We suggest that the irregular behavior of the current through our objects of study, namely PEG-Si, PAF-Si and Hydrogenated PEG-Si thin films as function of increasing relative humidity could best be analyzed for chaoticity using both time series analysis and detrended fluctuation analysis; this was applied both to the entire data and binned data according to both time and relative humidity intervals. Instances of chaotic behavior were observed.

The outline of thesis is as follows:

In chapter 2, a short introduction to dynamical systems containing material that we shall use later for the characterization of chaoticity in systems sampled as a time series of a single signal, such as mutual information, delay time, false nearest neighbors and lyapunov exponents are explained. The delay times were investigated using the average mutual information, the embedding vectors were constructed using embedding dimension values from the method of false nearest neighbors and maximal Lyapunov Exponents were first obtained for the Lorenz time series as an example.

In chapter 3, the transient current through thin films of PEG-Si, PAF-Si and Hydrogenated PEG-Si, all known to have irregular current characteristics under constant voltage and slowly varying relative humidity were studied. Possible chaotic behavior in the transient current can come from either the behavior of the relative humidity as a function of time or from the physical properties of the sample. We studied the

time behavior of the relative humidity for the pure PEG case and the PAF and Hydrogenated PEG cases. The time behavior of the relative humidity can be modelled by the absorption of the humidity introduced into the chamber by the sample. Using these results, we have decided to investigate the chaotic behavior of PEG-Si sample under varying humidity by binning the transient current data into ranges dictated by the relative humidity values instead of the time, since the increase in relative humidity is not linear.

In chapter 4, we use Detrended Fluctuation Analysis to confirm the chaoticity in our samples. This is a scaling analysis method used to estimate long-range, power-law correlation exponents. We studied long-range correlations in fluctuations of the transient current through PEG-Si, PAF-Si and Hydrogenated PEG-Si.

In chapter 5, the results of this investigation are discussed.

2. DYNAMICAL SYSTEMS

The object of study is a one dimensional signal S(t) that evolves in time and represents the transient current through a thin PEG film. This signal is assumed to come from a dynamical system of m dimensions with a characteristic time scale or many time scales if the system is multi periodic.

The dynamical quantity that we are observing can depend implicitly on time through the variables of a dynamical system xi. Let us assume that the basic dynamical system whose state vector is $x = x_i \in R^n$

$$\frac{dx}{dt} = f_i(x_0(t), x_1(t), ..., x_n(t)), f_i \in R^n \rightarrow R^n, i = 0, 1, 2, ..., n \tag{2.1}$$

with given $x_i(t_0)$(initial value problem) for n state variables.

The time evolution of the dynamical observable S(x_1, x_2, ...) thus depends on that of x_i. By using a Taylor expansion, we have:

$$S(T + t) = S(t) + T\frac{dS}{dt} + ... \tag{2.2}$$

All time derivatives can be evaluated using the chain rule and the dynamical system

$$\frac{dS}{dt} = \frac{\partial S}{\partial t} + \frac{\partial S}{\partial xi}\frac{\partial xi}{\partial t} \tag{2.3}$$

$$\frac{dS}{dt} = \frac{\partial S}{\partial t} + f_i\frac{\partial S}{\partial x_i} \tag{2.4}$$

with obvious generalization for higher order.

Since our signal is sampled at discrete time intervals, we actually use the notation $x_i((n+1)t) = x_i(nt) + tf_i(x_0(nt), x_1(nt), .., x_n(nt))$, for i= 0, 1, 2, .., n for variables sampled at discrete times nt. Since the functions fi do not depend on time explicitly, the above definition of the dynamical system is called an autonomous system of equations for x_i. If the system is not autonomous, we can trivially augment the system by an additional variable $x_n + 1$ without loss of generality.

We see that the one dimensional signal actually contains information about the dynamical system. In order to extract this information two parameters are significant here. One is the choice of t so that the one term Taylor expansion is meaningful, the other is the number of terms x_i that we need to process in order to extract reliable information on the derivative $\frac{\partial S}{\partial x_i}$.

The method of time delay embedding which is based on a delay time t and an embedding dimension m is the most important phase space reconstruction technique that takes these two points into consideration. This method reconstructs the dynamics of a possible basin of attraction by using delay coordinates from state space vectors S_i. For N point time series $s_1, s_2, s_3, ..., s_N$ the reconstructed state of the system at time segment i represented as $s_i = [s_i, s_{i+t}, ..., s_{i+(m-1)t}]$. Here t is the reconstruction delay or lag and m is the embedding dimension.Here the constructed trajectory S and t is given by the sequence of vectors $S = [s_1, s_2, s_3, ..., s_m]$. Time delay embedding provides a one-to-one image of the original set, provided m is large enough to embed. According to Taken's Theorem, a reliable reconstruction, i.e., an embedding, is guaranteed as long as the embedding dimension is greater than twice the topological dimension, n, m $>$ 2n [1, 2, 15]. We can understand this by a simple example. We need the value of a quadratic function at three different points to construct it. A reliable reconstruction refers to one that preserves the system invariants, e.g., fractal dimension and lyapunov exponents. In order to keep the size of the time series manageable, the data are occassionally split into bins and processed.

In experiments, i.e., with noisy and finite data sets, a value of t that is too small results in little information gain between successive delay coordinates and dis-

regards possible periodicities; the reconstructed trajectory becomes compressed along the main diagonal, or identity line of the embedding space. With chaotic systems and large values of t, successive delay coordinates may become casually unrelated, and the reconstruction is no longer representative of the true dynamics. In particular, if t happens to coincide with one of the periods of this system, a spurious stationarity would be introduced. The value of t, namely the delay to use when embedding, can be estimated by one of the following criteria: the first minimum of the mutual information or the first zero of the autocorrelation function. The former is preferable, since it takes into consideration nonlinearities.

2.1. Autocorrelation Function

A way of determining a suitable time lag for the signal S is calculating the first minimum of the autocorrelation function of the time series. We begin by calculating the mean $\bar{S}$

$$\bar{S} = \frac{1}{N} \sum_{m=1}^{N} S(m) \tag{2.5}$$

The autocorrelation function is defined as follows:

$$A(t) = \frac{\frac{1}{N} \sum_{m=1}^{N} \left(S(m+t) - \bar{S} \right) \left(S(m) - \bar{S} \right)}{\frac{1}{N} \sum_{m=1}^{N} \left(S(m) - \bar{S} \right)^2} \tag{2.6}$$

While the first zero or minimum of the autocorrelation function gives a reasonable value for time delay, it should be remembered that the autocorrelation function involves variances so that a nonlinear model would introduce spurious residuals and misestimate the delay time. The autocorrelation function is based on the linear dependence between a signal and a delayed verison of it in least squares sense on the average [3, 4, 5]. In other words, it describes the similarity between observations as a function of time seperation between them. Hence the first zero crossing of the autocorrelation function indicates the independency of the current observation from that after t time steps, thus giving a reasonable estimate for the delay time.

Autocorrelation based methods have the advantages of short computation times particularly when calculated via FFT. As suggested a particular criterion may be superior for one dynamical system and poor for another so mutual information is suggested by Fraser and Swinney [20].

2.2. Mutual Information

In contrast to the linear dependence measured by the autocorrelation, mutual information I(t), provides a measure of general dependence. Therefore I(t) is expected to provide a better measure of the transition from small t to large t with nonlinear systems. Mutual information answers the following question; given the observation of S(T), at time T, how accurately can one predict S(T+t) after a delay of t, so that successive delay coordinates are interpreted as relatively independent when the mutual information is small? Let us assume that there exists two sets X and Y with x_i being the possible outcomes of a measurement on X and y_j the possible outcomes of a measurement on Y. If the measurement x_i is completely independent from y_j then

$$P_{XY}(x_i; y_j) = P(x_i)P(y_j) \tag{2.7}$$

The joint probability of observing x_i by a measurement of X and observing y_j by a measurement of Y, $P_{XY}(x_i; y_j)$, should be different from the product of the individual probabilities of measuring x and y out of the sets X and Y respectively, $P(x_i)$ and $P(y_j)$, if there is correlation between the two sets. The logarithm of that ratio in bits is therefore called the average mutual information of X and Y as below;

$$\log_2 \frac{P_{XY} x_i; y_j}{P(x_i)P(y_j)} \tag{2.8}$$

The weighted average of the average mutual information is given by the following formula [5, 11]:

$$I(X;Y) = -\sum_x \sum_y (P_{XY}(x_i; y_j)) \log_2 \frac{P_{XY}(x_i; y_j)}{P(x_i)P(y_j)} \tag{2.9}$$

To apply this formula to time series analysis, we assume that S(n) as Set X and S(n + t) as Set Y. Here we obtain the average mutual information as below

$$I(t) = -\sum_{x}\sum_{y}(P(s(n+t), s(n)) \log_2[\frac{P(s(n+t), s(n))}{P(s(n+t))P(s(n))}] \tag{2.10}$$

It is very natural to take time delay as a multiple of the sampling time of the time series. If the time delay is taken too short then components of the reconstructed vectors will be close to each other, causing the state space picture to appear on the diagonal line, therefore we will have loss of information about the real system. On the other hand using a too long delay time will cause the correlations between the components of reconstructed vectors to be lost and signals are mistakenly recognized as random [3].

We obtain the mutual information vs time graph to decide the suitable delay time [4, 5]. As an example, the time evolution of the Lorenz attractor data, which will be given in the next subsection in detail, is investigated in order to find the value of a suitable choice of a time lag for calculation of the dimension of the attractor of the system more accurately. As t gets large the behavior of the signal makes the measurements independent hence the Mutual Information I(t) goes to a minimum, preferably zero. Using the first minimum of the Mutual Information vs time graph as delay time gives the value of 15 seconds.

In this graph of the mutual information, I(X;Y) , I(t) starts off very high (given a measurement S(t), we know as many bits as possible about $S(t + \sigma) \approx S(t)$, for σ zero or very small). As σ is increased, $I(\sigma)$ decreases, then usually rises again. If we recall that the largest Lyapunov exponent is 2.16 and the next one is nearly zero, such behavior is understandable. It is suggested that the value of time delay where $I(\sigma)$ reaches its first minimum be used for the state space reconstruction [20].

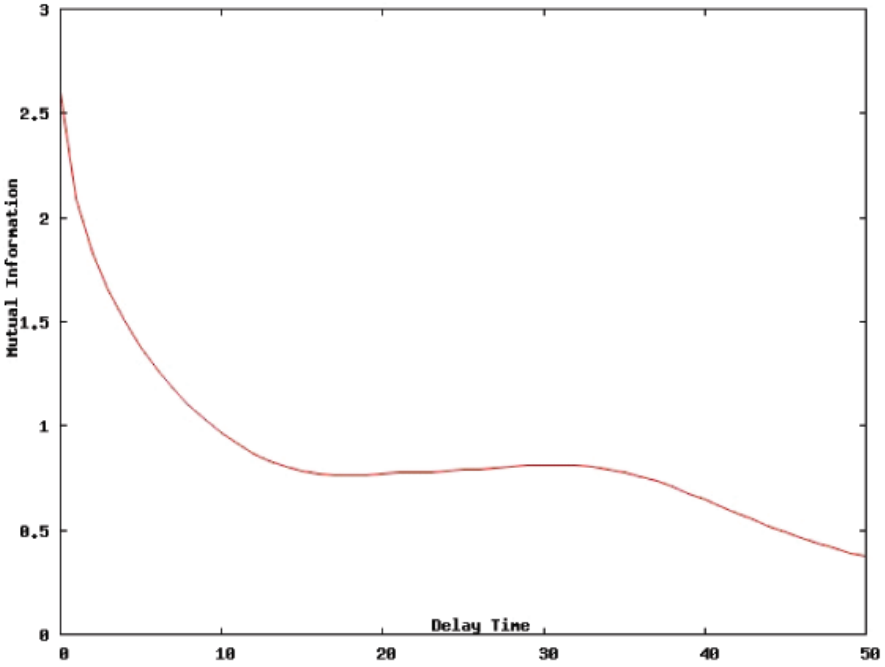

Figure 2.1. Mutual Information vs Delay time of the Lorenz data.

2.3. Embedding Dimension

Most of the systems in nature wander chaotically on a set of points called strange attractors. The strange attractor for the Lorenz system [6]

$$\frac{dx(t)}{dt} = s(y - x) \tag{2.11}$$

$$\frac{dx(t)}{dt} = -y - zx + ax \tag{2.12}$$

$$\frac{dx(t)}{dt} = xy - bz \tag{2.13}$$

with parameters s=10 ,a=28, b=8/3, is shown in Figure 2.2.

A related difficulty with attractor reconstruction involves the choice of the em-

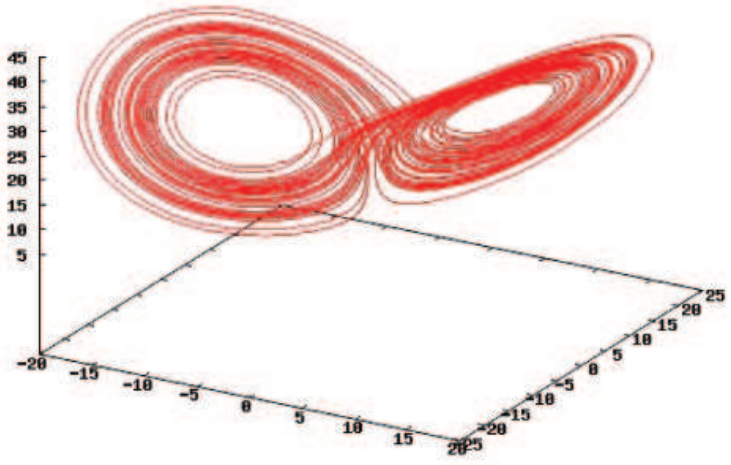

Figure 2.2. Strange attractor for Lorenz system.

bedding dimension, m. After choosing an acceptable time delay we need a sufficiently large embedding dimension for the reconstructed phase space that avoids projecting the system onto a lower dimensional space. As mentioned before, the embedding theorem [1, 2, 6] tells us that if the box counting dimension of the attractor defined as n, an embedding dimension m that is greater 2n, will absolutely allow unfolding the system in the reconstructed phase space. Normally, one has no a priori knowledge regarding the topological dimension, and it is unclear what a proper value of m would be. Here we consider the Lorenz system that has a phase space behavior shown in the figure. The box dimension of the Lorenz attractor, n is known to be 2.06. This box counting dimension implies choosing the embedding dimension m as 5.

One needs a criterion for the minimum embedding dimension, suffcient to unfold the attractor. At this point the false nearest neighbors method is a useful tool to give an estimate for the embedding dimension. Suppose that a space reconstruction in dimension $m > m_0$ is carried out, where m_0 is the minimum dimension that unfolds the reconstructed attractor. In m - dimensional space the reconstructed attractor becomes a one to one image of the attractor in the original phase space. Conservation of the topological properties of the actual phase space satisfies mapping neigboring points of

a given point of the original system onto neighbors of the image of that given point in the reconstructed space [5]. This is usually understood as equivalent tangent spaces.

Beginning with the reconstructed data vectors in m dimensions with a proper time lag t , and the time delay vector

$$y(k) = \left[s_{(k)}, s_{(k+t)}, ..., s_{(k+(m-1)t)}\right] \tag{2.14}$$

$y \in R^m$ in the embedded system with embedding dimension m, the nearest neighbors in phase space of the vector will be another time delay vector,

$$y_{NN}(k) = [s_{NN(k)}, s_{NN(k+t)}, ..., s_{NN(k+(m-1)t)}] \tag{2.15}$$

Here $y(k)$ and $y_{NN}(k)$ are real embedded space neighbors so that they are presumed to arise from original neighbors of the dynamics of the system. As in the choice of time delays [8], if we chose an embedding dimension not large enough then the attractor will not unfold properly and because of the projection, false data points that are not neighbors will fall into each others neighborhood. Hence an increase in the embedding dimension will cause a decrease in the number of false neighbors, until we have taken a sufficiently large embedding dimension so that the decrease in the number of neighbors stabilizes.

Let R_d be the Euclidean distance between $y(k)$ and $y_{NN}(k)$ in m dimensions defined as

$$\|y(k) - y_{NN}(k)\|^2 = R_m^2 \tag{2.16}$$

$$\|y(k) - y_{NN}(k)\|^2 = \left[[s_{NN}(k) - s_{(k)}]^2 + ... + [s_{NN(k+(m-1)t)} - s_{(k+(m-1)t)}]^2\right] \tag{2.17}$$

In m+1 dimension y(k) becomes $[s_{(k)}, s_{(k+t)}, ..., s_{(k+(m-1)t)}, s_{(k+(m-1+1)t)}]$, $y \in R^{m+1}$ and the distance between points embedded in m+1 dimensions,$R_{m+1}(k)$ can be ex-

pressed in terms of $R_m(k)$ as

$$(R_{m+1}(k))^2 = (R_m(k))^2 + (s_{NN(k+(m)t)} - s_{(k+(m)t)})^2 \tag{2.18}$$

From this result we can define a threshold value $R_T(k)$

$$\frac{[s_{NN(k+(m)t)} - s_{(k+(m)t)}]}{R_m(k)} > R_T(k) \tag{2.19}$$

so that points that satisfy this condition are assumed to be neighbors in m dimensions but not so in m+1 dimensions. Such points are defined as false neighbors. For the Lorenz attractor, the minimal embedding dimension found by the method of false neighbors is three. We can conclude from this result that if the embedding dimension exceeds three, there will be no false neighbors and the attractor will be unfolded in greater than or equal to three dimensions [3, 8, 11, 14].

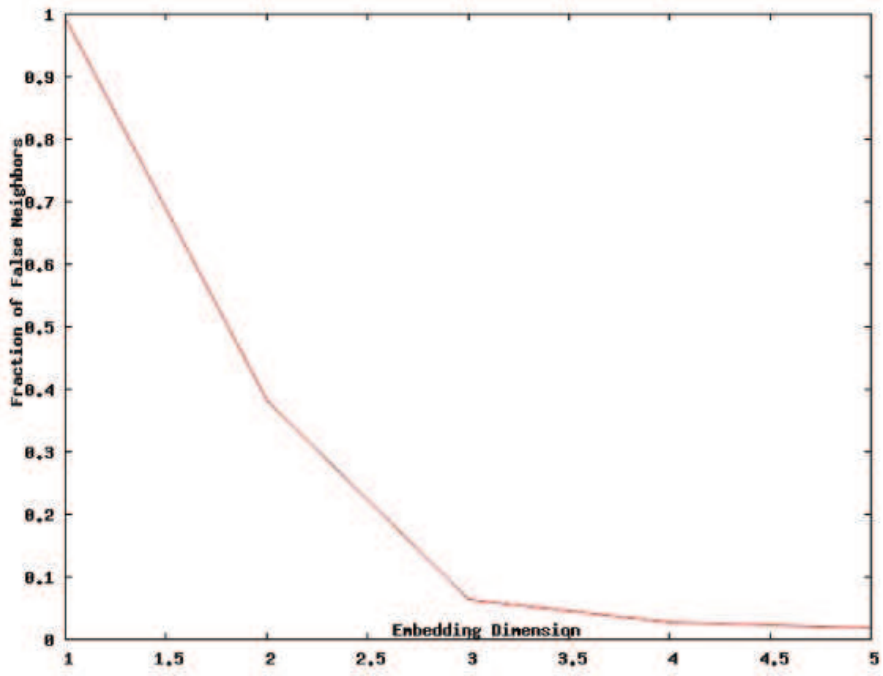

Figure 2.3. Embedding Dimension for Lorenz Series.

Results of the false neighbors calculation for this system are shown in Figure 2.3. We see that stabilization occurs if the embedding dimension is somewhere between 3 and 4. Therefore, depending on the system, one does not always have to use an

embedding dimension that is greater then two times the embedding dimension of the actual attractor.

2.4. Lyapunov Exponents

Lyapunov exponents measure the exponential rate at which nearby trajectories diverge or converge in time. There are as many Lyapunov exponents as there are dimensions in the state space of the system. Roughly speaking the (maximal) Lyapunov exponent is a time constant for the distance between two nearby orbits. A negative value for a Lyapunov exponent indicates that the orbits converge in time, thus shrinking in that direction. If all Lyapunov exponents are zero or negative, the dynamical system is insensitive to initial conditions If a Lyapunov exponent is positive, then the distance between nearby orbits grows exponentially in time, the orbit stretches in that direction and the system exhibits sensitive dependence on initial conditions. The largest Lyapunov exponent is usually the most important one since a positive value for it is one of the most common signals of chaotic behavior [7, 8]. If a system has a positive Lyapunov exponent but the sum of Lyapunov exponents is negative, then the state space of the system shrinks, but the orbit stretches in a particular direction, thus forming an attractor.

There are basically two ways to compute Lyapunov exponents. In one way one chooses two nearby points, allow them to evolve in time, measuring the growth rate of the distance between them. This is useful when one has a time series, but has the disadvantage that the growth rate is really not a local effect as the points separate. A better way is to measure the growth rate of tangent vectors to a given orbit.According to the first method, to find the maximal Lyapunov exponent, one chooses a point s_{n_0} and its neighbors. One then considers the representation of the time series data as a trajectory in the embedding space; trying to observe a very close return $s_{n_0}{}'$ o a previously visited point s_{n_0} By very close, we understand that the points lie in a hyperbox consisting of a hyperball of size ϵ, whose size as a function of the time or number of iterations in the time series, is the stretching factor. By computing the average over distances of all neighbors to the reference point s_{n_0} as a function of relative

time, taking the logarithm of the distance of a slightly perturbed orbit and averaging over the trajectory, we find the maximal Lyapunov exponent as shown below;

$$s\left(\Delta n\right)=\frac{1}{N}\sum_{n_0=1}^{N}In\left(\frac{1}{|U(s_{n_0})|}\sum_{S_n\varepsilon U(s_{n_0})}|s_{\Delta n+n_0}-s_{\Delta n+n}|\right) \tag{2.20}$$

Here s_{n_0} is reference point that can be assumed as embedding vectors. $U(s_{n_0})$ is the neighborhood of s_{n_0} . A reliable characterization requires independence of embedding parameters and the exponential law for the growth of distances are checked explicitly. Based on this understanding, one can derive a robust consistent and unbiased estimator for the maximal Lyapunov exponent. If the graph of $s(\Delta n)$ vs Δn results in a robust increase, its slope is assumed to estimate the maximal Lyapunov exponent [7].

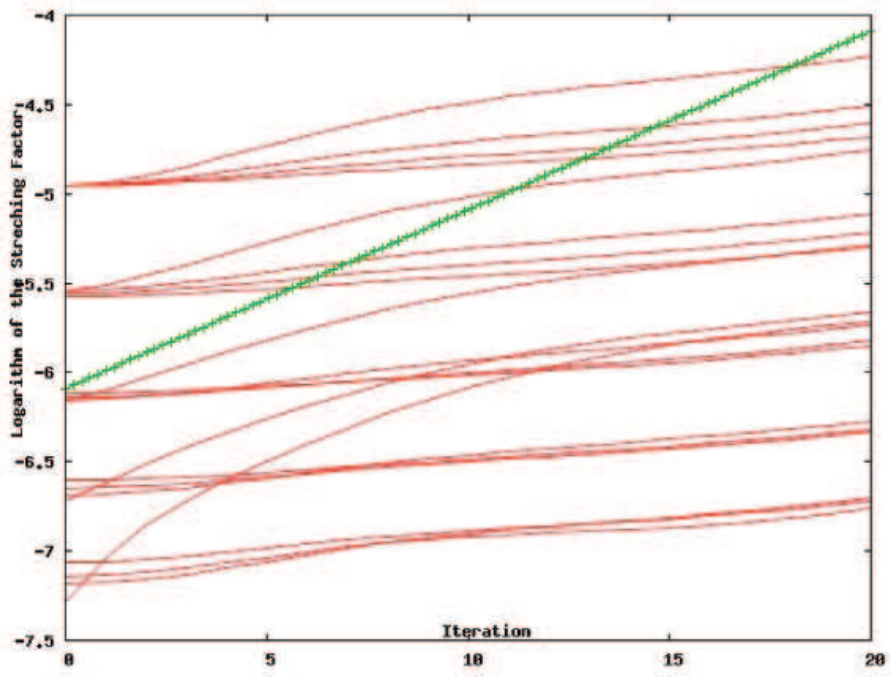

Figure 2.4. Lyapunov Exponents vs Iteration.

Results of the Maximal Lyapunov Exponent calculation for this system is shown in the Figure 2.4. In the graph for different epsilon, values, ϵ, there are number of points for which a neighborhood with enough points can be found. We select the neighbors with distance smaller than ϵ represented as $U(s_{n_0})$. After m = 3 characteristic properties of the lines change and exponentially diverge from the original basin so m =

3 is a suitable choice for the embedding dimension in this calculation. From the graphs of the streching factor $s(\Delta n)$ vs Δn, there is a robust linear trend for all ϵ values. We can conclude from this result that the maximal Lyapunov exponents [1/unit time] is 0.906. The Tisean program [5, 7] can also calculate the full set of Lyapunov exponents and the remaining ones are found to be 0 and -14.572.

3. CHARACTERISTICS OF THE TRANSIENT CURRENT DATA IN THE PEG-Si SAMPLE

Polymers with hydrophilic properties have been used in humidity sensor devices. Hydrophilic groups such as - $COOH$ and - SO_3H are perfect materials for sensors. At high humidity levels, such polymers cease to work properly in sensors because of their solubility in water. A hydrophilic molecule is one that is typically charge-polarized and capable of hydrogen bonding since they can dissolve more readily in water than in other hydrophobic solvents. Hydrophilic and hydrophobic molecules are polar molecules and nonpolar molecules, respectively. These problems have been overcome by mixing the hydrophilic materials with hydrophobic ones or using hydrophobic polymers with hydrophilic branches by crosslinking the hydrophilic polymers with a suitable substance.

Poly(ethylene glycol) (PEG), also known as poly(ethylene oxide) (PEO) or poly-oxyethylene (POE) is a hydrophilic polymer and crosslinked with Gama-isocyanat-rophyltriethoxysilane to obtain PEG - Si Thin Films. Hydroxyl ended PEG (4000 g/mole) is dissolved in technical toluene as a solvent in the synthesis. Afterwards the PEG Solution is refluxed in a dean-stark apparatus to remove the humidity kept in the polymer. After obtaining the dried PEG - Toluene Mixture, they are treated with Gama-isocyanatrophyltriethoxysilane overnight. The total solution is kept in ethanol and methanol mixture for one day. To obtain the PEG-Si Films, a glass substrate is immersed into this solution for dip-coating of the polymer thin film and then it is kept fixed as the polymer solution is free to flow with constant speed. After these operations, the polymer coated glass substrate is dried and kept in an oven for crosslinking between substances. The other method is one in which the glass substrate is kept fixed and the solution is dropped directly and then it is dried untill crosslinking of the thin film on the scratched glass substrate is complete [19].

These prepared samples are enclosed into a closed chamber with some saturated salt KNO_3 to increase the relative humidity and $ZnCl_2$ to decrease the relative humidity in the chamber. After placing the salts, the relative humidity change and the corresponding voltage change is recorded by the the humidity sensor. Both the current and the humidity values were read by computer - controlled ammeters. The change in the humidity has an accuracy of 2 per cent taken by the sensor when a dc electric field is applied to the polymer sample that measures the current through it. The humidity sensor records the varying relative humidity versus electrical current in the PEG sample at uniform time intervals [19].

A typical current versus time graph is shown below in Figure 3.1. abd the current versus relative humidity graph is shown below in Figure 3.2. Either figure suggests that chaotic behavior is possible. The form of the data makes either time series analysis or detrended fluctuation analysis feasible.

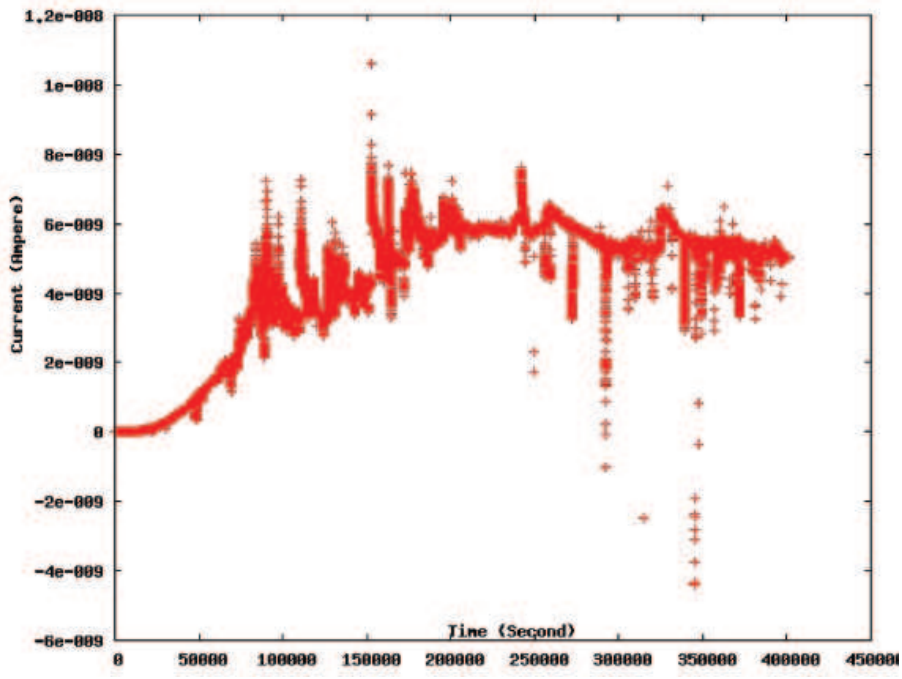

Figure 3.1. Pure PEG Sample Current vs Time.

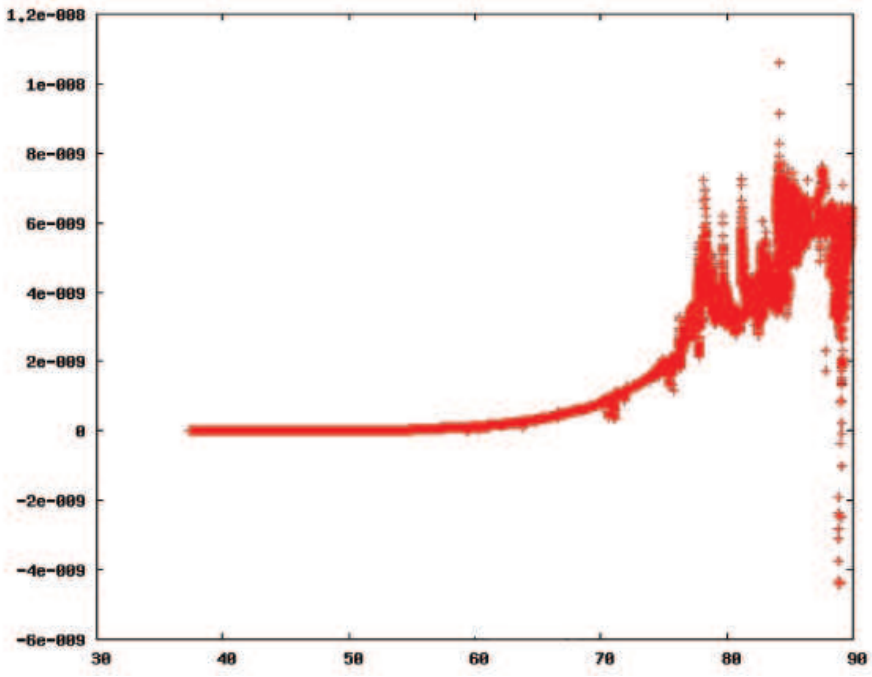

Figure 3.2. Pure PEG Sample Current vs Relative Humidity.

3.1. Analysis of the Time Dependence of Relative Humidity

Before embarking on the analysis of chaotic behavior in the current, there is an important question that needs to be answered. Possible chaotic behavior in the transient current can come from either the behavior of the relative humidity as a function of the time or from the physical properties of the sample. The former is likely to create an obvious complication. To answer this question, we embark on a study of the time behavior of the relative humidity for the pure PEG case and the PAF and Hydrogenated PEG cases that will be studied subsequently, since the mechanism for introducing the humidity into the chamber is the same in all cases. We first examine the variation of the relative humidity as a function of time. As a first try, we assumed a simple exponential relaxation [9, 10]. The functional form that we use is

$$RH = a_1(1 - a_2 \exp(-\frac{t}{t_0})) \tag{3.1}$$

As we can see from the figure above, the form of the data suggests a relaxation

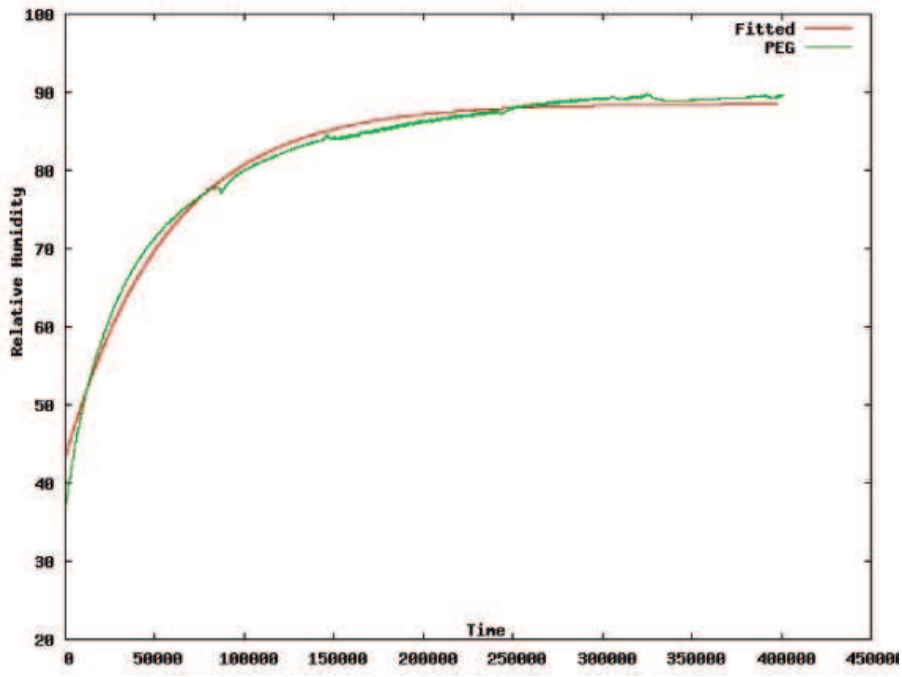

Figure 3.3. Relative humidity vs time overplotted with an exponential relaxation fit for PEG.

behavior. However, the residual chisquare per degree of freedom is 1.30498. with $a_1 = 88.523 \pm 0.003$, $a_2 = 0.5107 \pm 0.0007$, $t_0 = 56831.6 \pm 21.8$. The fit is unsatisfactory and contains systematic discrepencies as one can see from the Figure 3.3. showing the data overplotted with the fitted values.

A more promising possibility is a stretched exponential function. Such relaxation phenomena have been observed in diffusion phenomena with noise in [10]. Here although equilibrium is finally reached, the main trend is reflected by the stretched exponential function. The residual relative humidity is modelled by the product of an absorption coefficient a_2 and the stretched exponential function. The fit gave a residual chisquare per degree of freedom of 0.134048 and the functional form is

$$RH = a_1(1 - a_2 \exp(-(\frac{t}{t_0})^{\alpha}) \tag{3.2}$$

with the parameter values $a_1 = 90.3199 \pm 0.002$, $a_2 = 0.640363 \pm 0.00011$, $t_0 =$

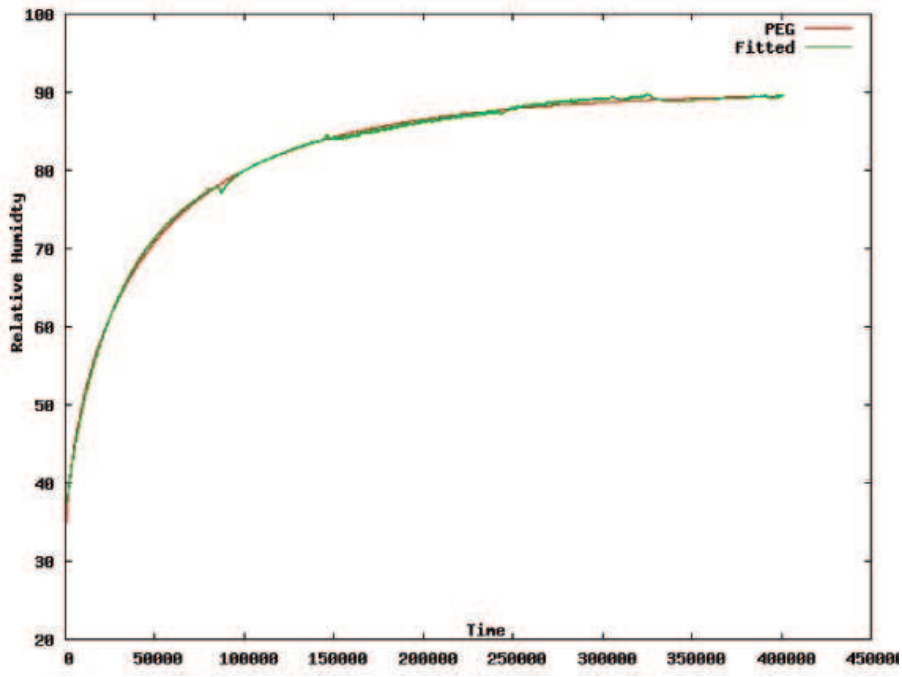

Figure 3.4. Relative humidity vs time overplotted with a stretched exponential relaxation fit for PEG.

43933.27 ±2.39, $\alpha = 0.661957 \pm 0.000176$.

The plot reveals that as evidenced by the very low chi squared per degree of freedom value, the fit is excellent and all systematic discrepancies have disappeared. It is known that [12, 13] many polymer molecules tend to absorb significant amounts of water when exposed to high humidity and the absorption can be modelled by a stretched exponential.

It is clear that the diffusion of water vapor into the chamber can be understood by absorbtion by the sample with an anomalous diffusion pattern. The residuals follow a characteristic narrowband noise pattern [9].

The measurement of the transient current was repeated after treating the PEG sample with alcohol to obtain PAF. The details will be given in Section (3.3) The variation of the relative humidity as a function of time is studied in a manner similiar to the PEG case. The simple exponential relaxation fit (Equation 3.1) gave a residual chisquare per degree of freedom of 0.141163 with $a_1 = 78.6483 \pm 0.0033$, $a_2 = 0.413474$

$\pm$ 0.000097, $t_0 = 9971.04 \pm 5.01$. Although the fit is better, it still contains systematic discrepencies as one can see from Figure 3.5. showing the data overplotted with the fitted values [11, 12, 13].

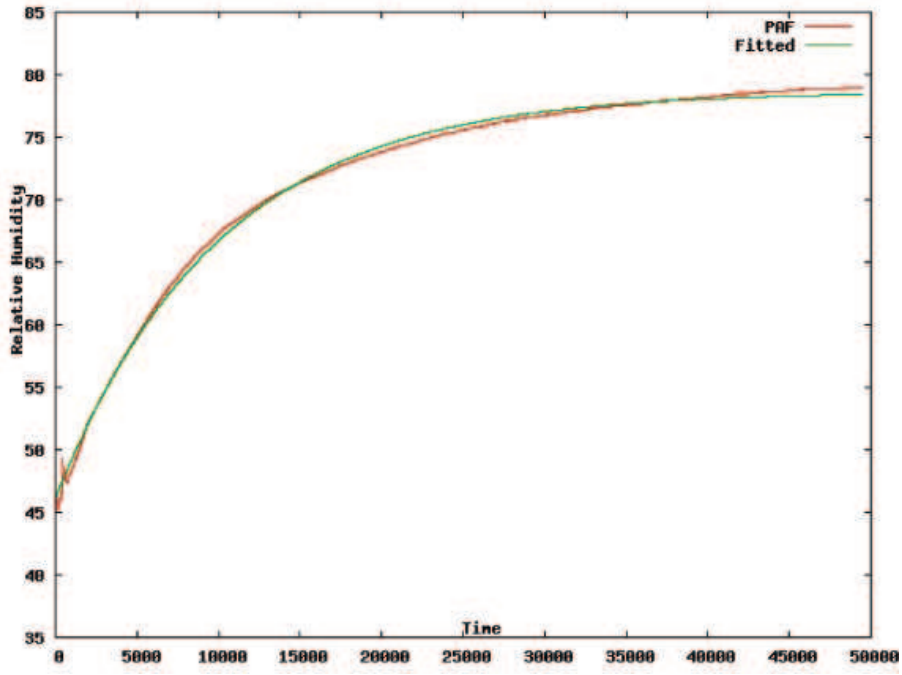

Figure 3.5. Relative humidity vs time overplotted with an exponential relaxation fit for PAF.

The stretched exponential function arrangement (Equation 3.2) gives an excellent fit where all systematic discrepancies have disappeared. The residual chisquare per degree of freedom is 0.054745, with the parameter values $a_1 = 79.3361 \pm 0.0038$, $a_1 = 0.444552 \pm 0.000146$, $t_0 = 2677.63 \pm 13.20$, $\alpha = 0.861039 \pm 0.000520$. This is shown in Figure 3.6.

The measurement of the transient current was further repeated after treating the PEG sample with hydrogen to obtain hydrogenated PEG. The details will be given in Section (3.3) The variation of the relative humidity as a function of time is studied in a manner similiar to the PAF and PEG cases. The simple exponential relaxation fit (Equation 3.1) gave a residual chisquare per degree of freedom of 0.529108 with $a_1 = 78.1262 \pm 0.0033$, $a_1 = 0.453048 \pm 0.000205$, $t_0 = 8307.97 \pm 6.12$. Although the fit is better, it still contains systematic discrepencies as one can see from Figure 3.7.

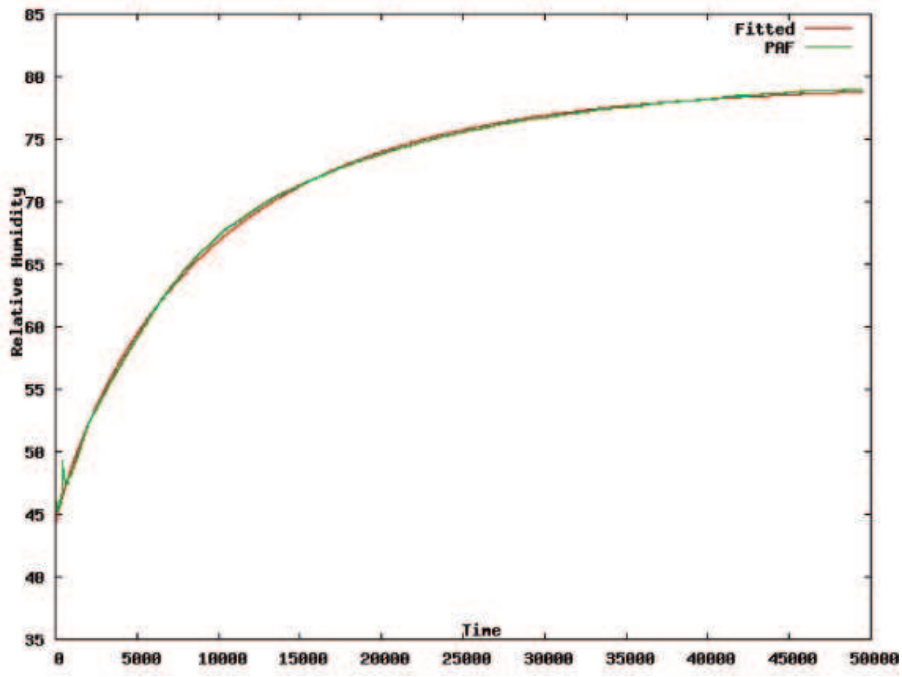

Figure 3.6. Relative humidity vs time overplotted with a stretched exponential relaxation fit for PAF.

showing the data overplotted with the fitted values [11].

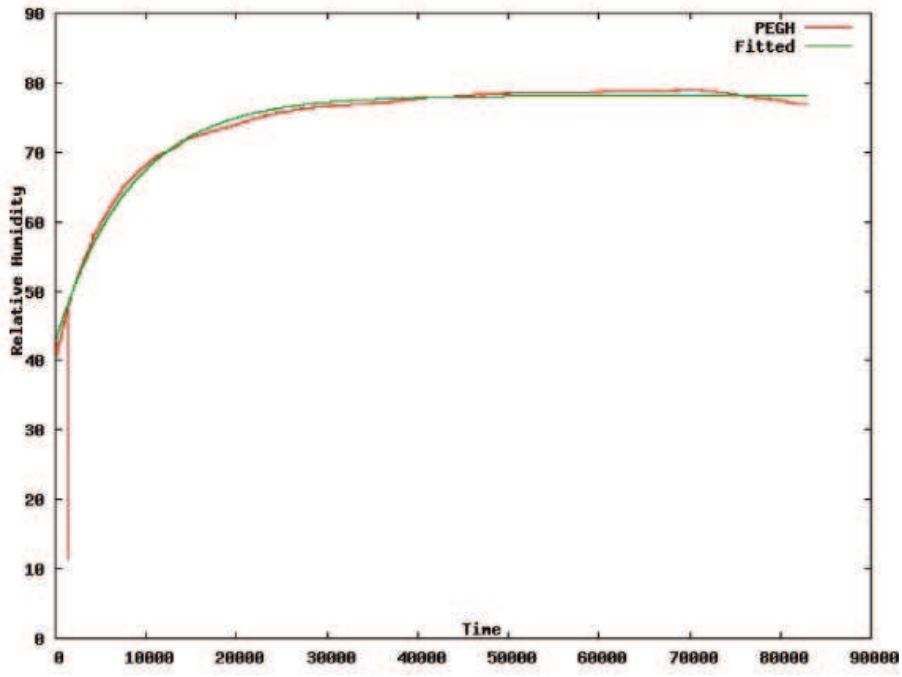

Figure 3.7. Relative humidity vs time overplotted with an exponential relaxation fit for hydrogenated PEG.

The stretched exponential function arrangement (Equation 3.2) again gives an excellent fit where all systematic discrepancies have disappeared. The residual chisquare per degree of freedom is 0.295029, with the parameter values $a_1 = 78.4868 \pm 0.003205$, $a_2 = 0.515505 \pm 0.000359$, $t_0 = 1067.98 \pm 8.598$, $\alpha = 0.787641 \pm 0.0008288$. This is shown in Figure 3.8.

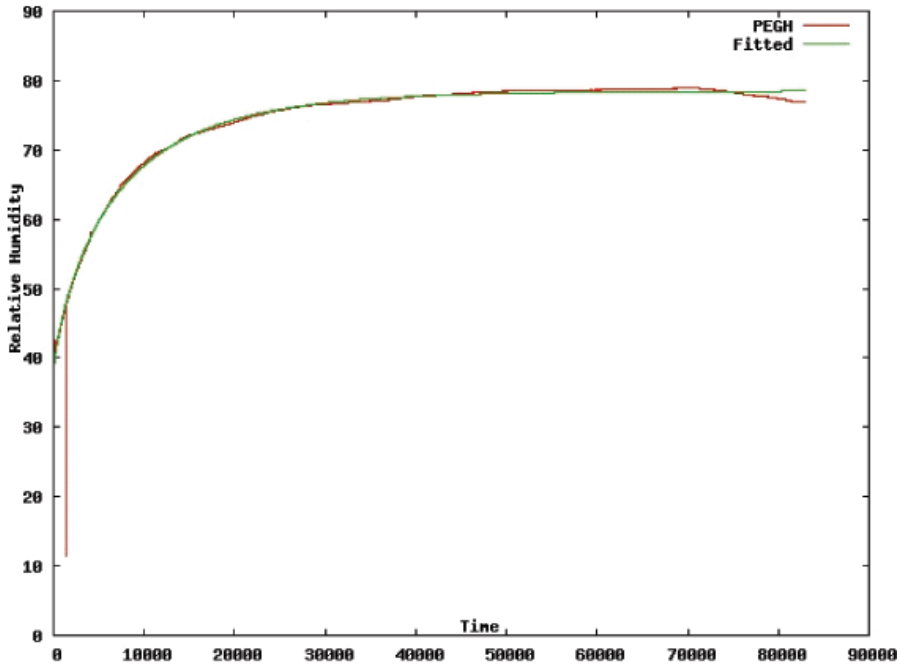

Figure 3.8. Relative humidity vs time overplotted with a stretched exponential relaxation fit for hydrogenated PEG.

We can conclude that the time behavior of the relative humidity can be modelled by the absorption of the humidity introduced into the chamber by the sample. Hence, any chaotic behavior that is identified is related to changes in the physical properties of the sample due to the absorption of humidity. There is one exception to this, for low relative humidity values, we do observe irregularities in the relative humidity versus time plot; this is probably due to the competition between the process of relative humidity being introduced into the chamber and the humidity being absorbed by the sample, before steady state sets in [11, 12, 13].

3.2. PEG - Si Analysis

In Figure 3.1 we observed an irregular current characteristic under constant voltage and slowly varying relative humidity at equal time steps for the pure PEG sample. In the actual experiment, it has been reported that after reaching a certain relative humidity level, a phase transition occurs from a semi crystalline state to a gel state [19]. Fluctuations in the elastic force relaxations and in the number of Hydrogen bonds is a likely cause for the irregularities observed in the time varying current [19]. One way to understand the irregular behavior of transient current through PEG-Si thin films is to use the fact that the time dependence of relative humidity is as explained in the previous section and take increasing relative humidity as a slowly varying parameter with the data split into equal time periods, 25,000 seconds.

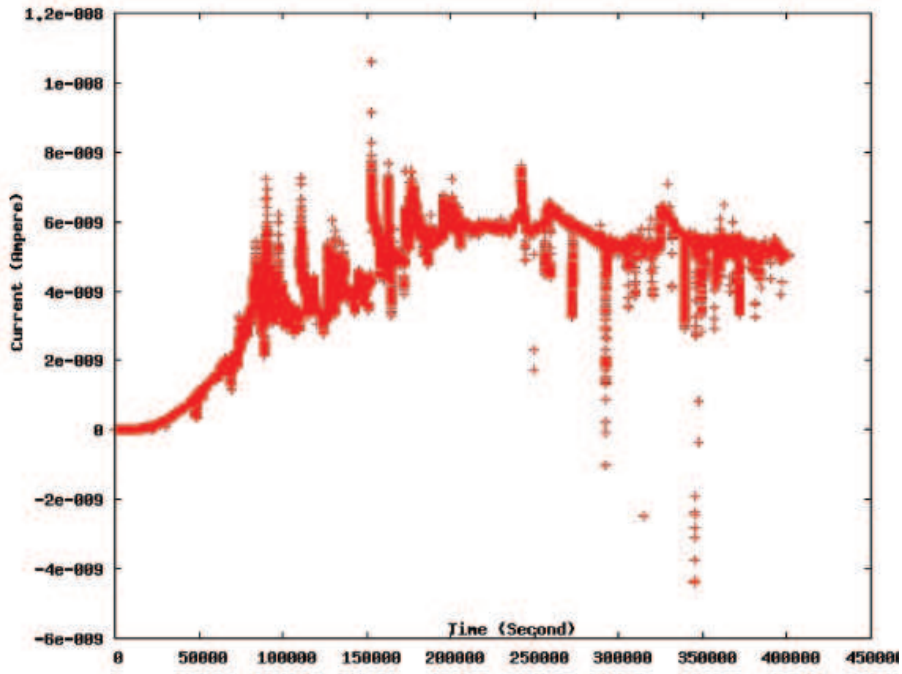

Figure 3.9. Pure PEG Sample Current vs Time.

After splitting the data into equal time periods, the delay times for data taken from the humidity sensor are analyzed using the Delay - Coordinate embedding theorem [1, 2, 3]. If the embedding is performed correctly, the theorem guarantees that the reconstructed dynamics of the system should be identical to the true dynamics of the system and dynamical invariants should also be identical. To work on time series at

first we build up delay vectors $(x(T), x(T+t), ..., x(T+(m-1)t))$. Here t and m represents delay time and the embedding dimension, respectively. The reconstructed invariants (basically, its fractal dimension and the maximal Lyapunov exponent) of the attractor as found by this approach remain invariant with respect to the unknown, original system that generated the series.

In order to find the value of the smallest embedding dimension m, we calculate the number of nearest neighbors. If one were to reduce the dimension of the actual attractor by one it could be that the attractor no longer represents the system and the points that are actually far apart become apparent neighbors, these are called false neighbors. As we increase the dimension of the embedding space one by one, the false neighbors should separate while the actual nearest neighbors should still remain so. Hence, as we increase m, the percent of nearest neighbors should fall down and eventually stabilize.

We define the mutual information as the measurement taken from the theory of information, and it also defines the probability with which the neighboring data points x_i and x_{i+t} are statistically independent. We have seen that, the function of mutual information I(X,Y) of two random variables X and Y measures the average amount of information about one random variable obtained from knowledge of the other and is given by Equation 2.9. [1, 5, 14].

The false nearest neighbors approach uses the property of the attractor which guarantees that there are no two orbits that intersect each other. If the attractor is reconstructed in a space with small number of dimensions, then as a result of the projection, some orbits intersect each other. In the case of discrete systems a number of points will crash upon each other indicating false closeness of path. The number and hence the fraction of false neighbors is defined as a function depending upon the embedding space dimension. For the desired embedded dimension we should have a fraction of false neighbors that is close to zero within some tolerance.

Turning this concept into an algorithm one would start with small values of m

and calculate the number of false neighbors generated. One would then increase the number of dimensions one by one until the number of false neighbors is zero or nearly zero. This means that this number of dimensions is the best embedding for the system - the one with the least dimensions required to correctly represent the system.

Three different methods exist for choosing the time delay, t. The first method is to choose the delay with which the phase portrait optimally fills the state space. The second method determines the proper time delay as the position of the first local minimum of the autocorrelation function of the data. Finally, the third method is to take the first minimum in the graph of average mutual information. While the first method makes a relatively rough estimation in a graphical procedure, and the second choice assumes a linear relation among successive points in the signal data, the mutual information method is the prefered method since it also takes into consideration possible nonlinear relations. The mutual information calculated by reconstruction of the state space for the PEG-Si current data gives the best estimate of the delay time for the data split into bins of equal time interval, giving a delay time of $t = 200$ seconds [5, 6, 26].

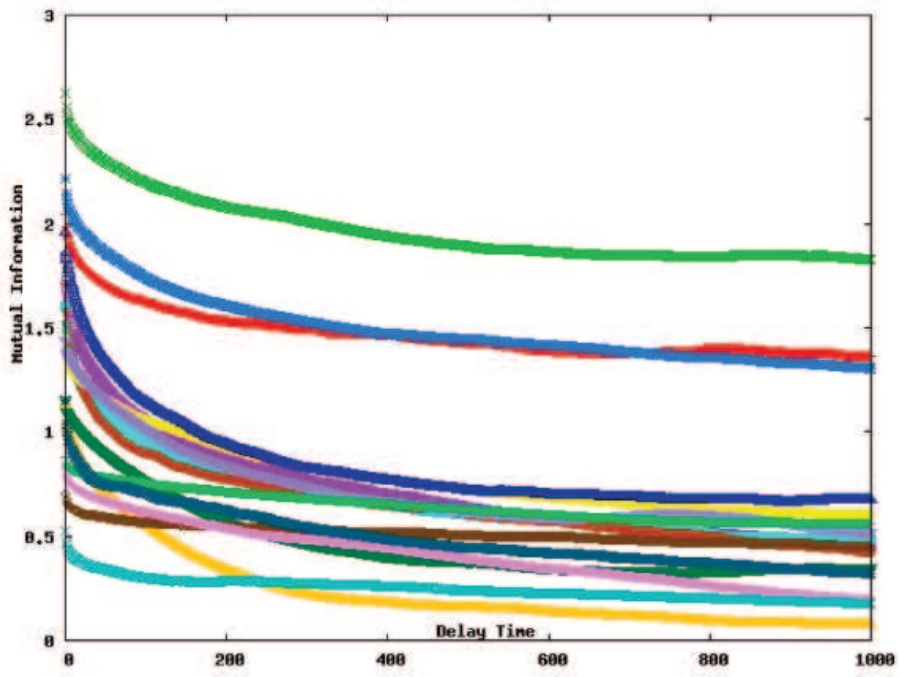

Figure 3.10. Mutual Information vs Delay Time for sets of data split into bins of equal time interval for PEG.

This figure describes the minimum time delay for all split data sets. The data show good agreement with the first local minimum in the graph of average mutual information and optimal filling of the state space as shown Figure 3.11.

Finding a good estimate of the lag or time delay is crucial for the calculation of the embedding dimension. For noise-free data, embeddings with different t but same m are mathematically the same. If t is small compared to the internal time scales of the system, successive elements of the delay vector are strongly correlated [9]. All vectors Sn are then clustered around the diagonal in R_m unless m is very large. If t is very large, successive elements are already almost independent and the points fill a large cloud in the Rm, where the deterministic structures are confined to the very small scales. For this experimental time series, this method indicates an embedding dimension of 12 if we are cautious about data that could possibly be corrupted by noise or any other factors [5, 6].

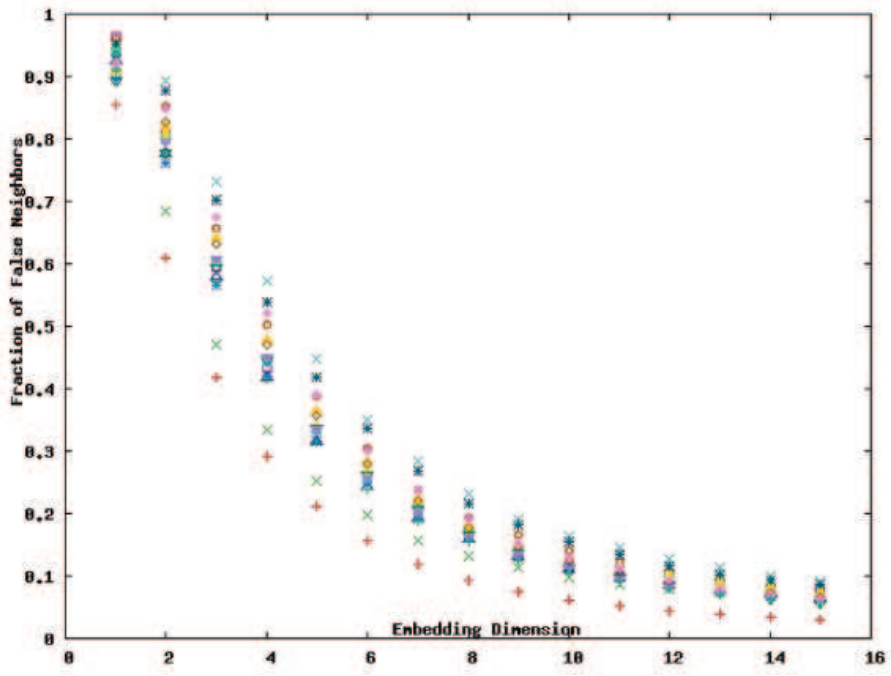

Figure 3.11. Embedding Dimension vs Fraction of False Neighbors for all split sets for PEG.

This figure describes the minimum embedding dimension to reconstruct the attractor as determined by the false neighbors method. Different shapes for the points

show different values of the time intervals. By supposing that a space reconstruction in dimension $m > 12$ is carried out, there will be no false neighbors and the attractor will be unfolded in greater than or equal to 12 dimensions. The embedding dimension appears to be independent of the relative humidity values [5].

Results of the Maximal Lyapunov Exponent calculation for this system are shown in Figure 3.12. In the graph for different epsilon values, ϵ, there are a number of points for which a neighborhood with enough points can be found. We select the neighbors with distance smaller than ϵ represented as $U(s_{n_0})$. After $m = 12$ characteristic properties of the lines change and exponentially diverge from the original basin so that this confirms $m = 12$ as a suitable choice for the embedding dimension in this calculation. From the graphs of the stretching factor $s(\Delta n)$ vs Δn, there is a robust linear trend for all ϵ values and slopes of the robust parts give positive values and identify chaotic behavior. The first graph represents a time range of 225000 to 250000 corresponding to a relative humidity range of 86.9 per cent to 87.6 per cent [6, 22].

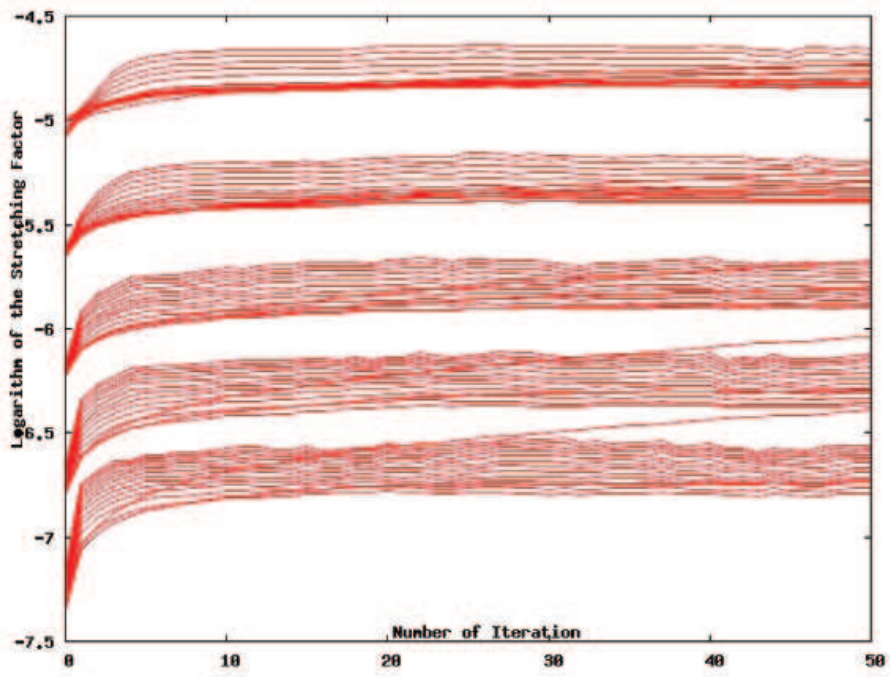

Figure 3.12. Number of Iterations vs Logarithm of the Strecthing Factor for PEG.

To ascertain that a positive maximal Lyapunov exponent can be seen at other values of the time range, a few further plots are presented. For relative humdities

between 70 per cent and 80 per cent we have approximately the same positive Lyapunov exponent value as shown in Figures 3.13, 3.14 and 3.15; The values range from 0.4567 to 0.6562. Since time bins of equal size contain varying amounts of change in the relative humidity because of the nonlinear dependence of the relative humidity on time, this analysis may not reveal the true dependence on the relative humidity. After 80 per cent relative humidity, we have a slight decrease in the values for the Lyapunov exponents. This may indicate an internal change in the system but differences are not large enough to allow us to make a precise statement as to the characterisation of a possible phase change in the system. Less noisy data would have been more helpful here [4, 5, 6]. An analysis based on relative humidity bins will be caried out below in order to clarify the situation.

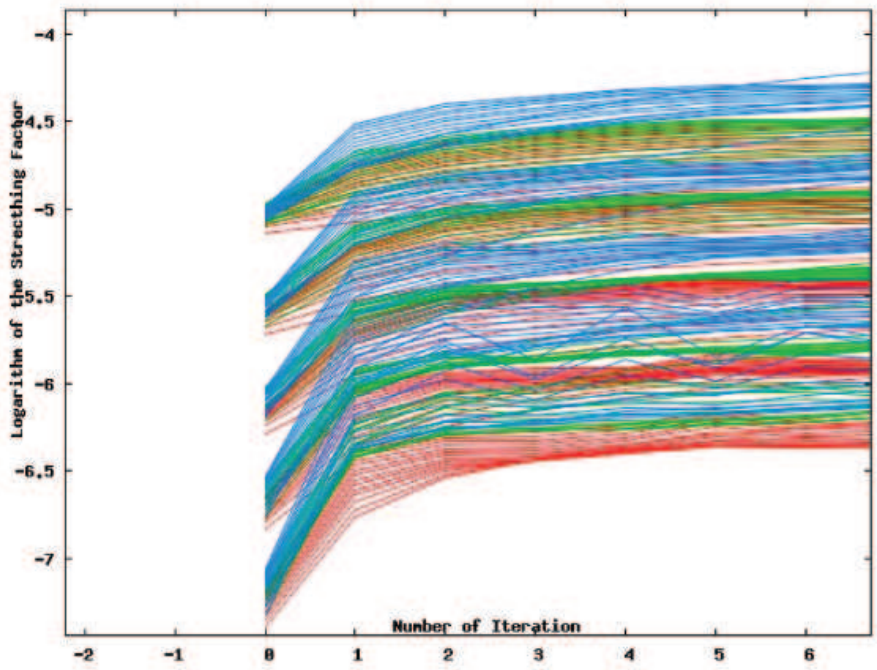

Figure 3.13. Lyapunov Exponents for relative humidities less then 70 per cent for PEG.

It is important to mention that quantitative analyses of chaotic systems are usually sensitive to not only the observation time, but also to the data size. From the previous graphs, it appears that the relative humidity acts as an order parameter. To see this more clearly, we have decided to investigate the Chaotic behavior of PEG-Si sample under varying humidity by binning the transient current data into ranges

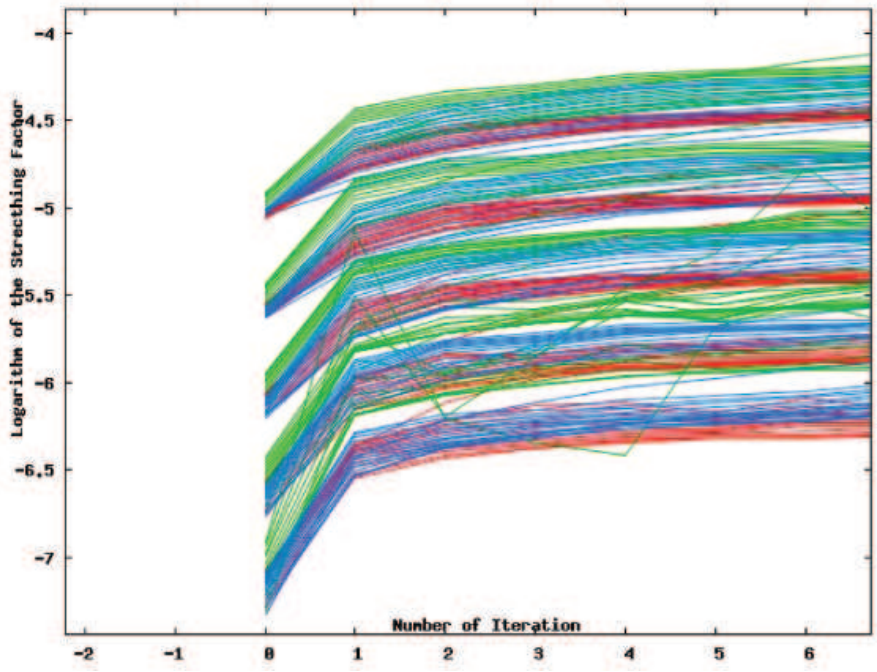

Figure 3.14. Lyapunov Exponents for relative humidities between 70 per cent - 80 per cent for PEG.

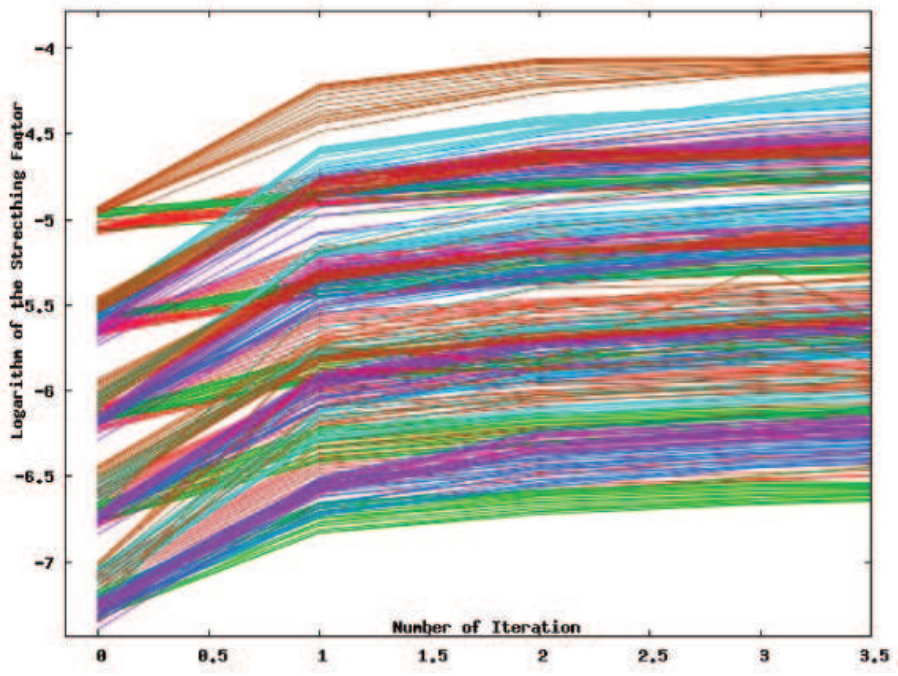

Figure 3.15. Lyapunov Exponents for relative humidities between 80 per cent - 90 per cent for PEG.

dictated by the relative humidity values instead of the time intervals. We split the relative humidity into 10 per cent bins. Unfortunately, relative humidity bins are not

of the same size since we have more than 400,000 data points and the most seemingly irregular part is between 80 per cent and 90 per cent. Therefore we split this range into 3% bins. Figure 3.16 shows the diagram for this analysis.

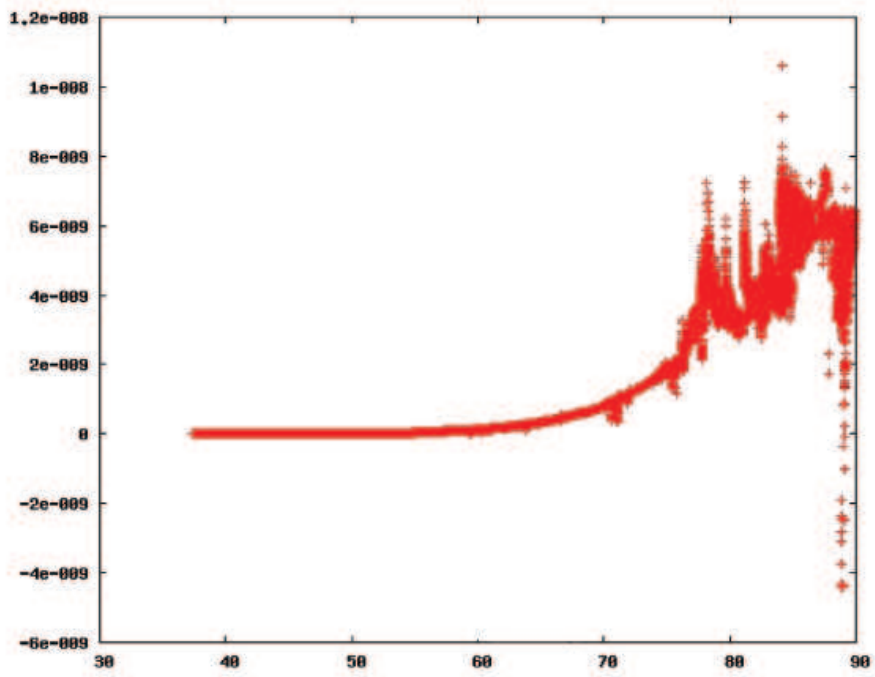

Figure 3.16. Pure PEG Sample Current vs Relative Humidity.

We have repeated the same procedure as above for this analysis, first delay time is calculated to obtain mutual information vs delay time graph. Different shapes for the points show different values of the relative hunmidity. As mentioned above we obtain approximately the same delay time for these data sets. Results are in Figure 3.17 showing the delay time of $t = 200$ seconds.

By taking the delay time as $t = 200$ seconds, we analyzed the minimum embedding dimension to reconstruct the attractor by the false neighbors method. Due to the fact that chaotic systems are stochastic when embedded in a phase space that is very small to accommodate the true dynamics, we choose the embedding dimension 12 as in the previous analysis. One may choose the smallest embedding dimension that yields a convergent result. Therefore as shown in Figure 3.18, there is no significant difference between relative humidity vs current and relative humidity vs time analyses to find the minimum embedding dimension.

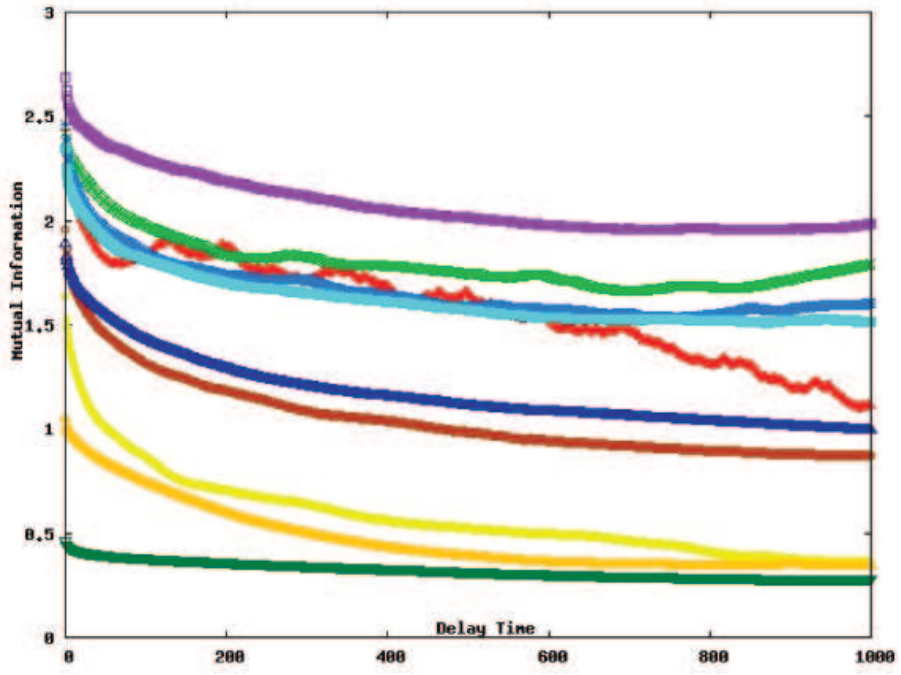

Figure 3.17. Mutual Information vs Delay Time for all split sets for PEG.

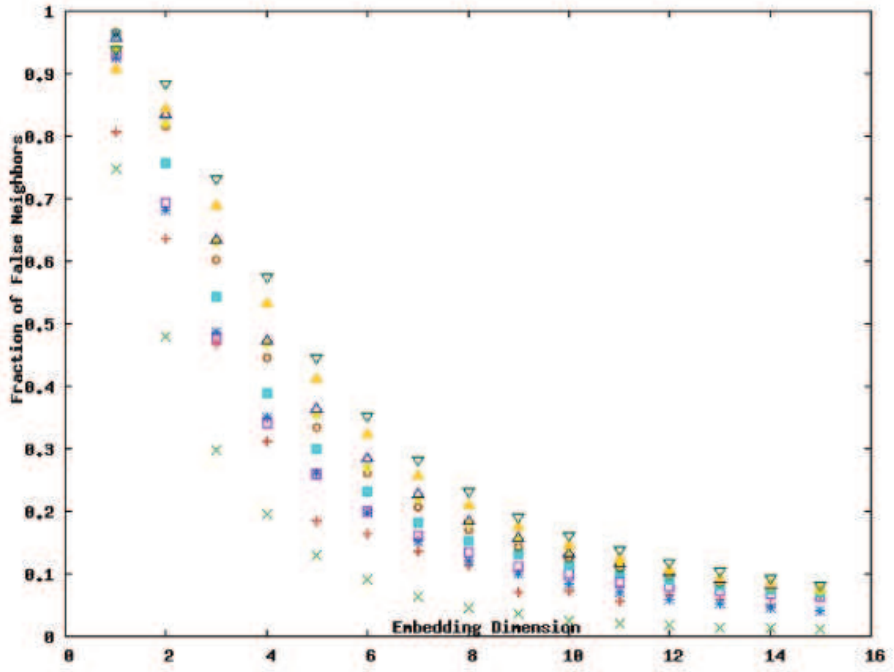

Figure 3.18. Embedding Dimension vs Fraction of False Neighbors for PEG.

The Lyapunov exponent calculation graphs are presented in Figures 19, 20, 21; we can observe that relative humidity vs current analysis have the maximal Lyapunov exponents 0.266704, 0.2103293, 0.228503, 0.448784, 0.540593, 0.526684, 0.517707, 0.3254; They are increasing up to 70 per cent relative humidity then they stabilize between 70

per cent and 86 per cent after which point we see a small decrease in the Lyapunov exponents [1, 5, 6, 7].

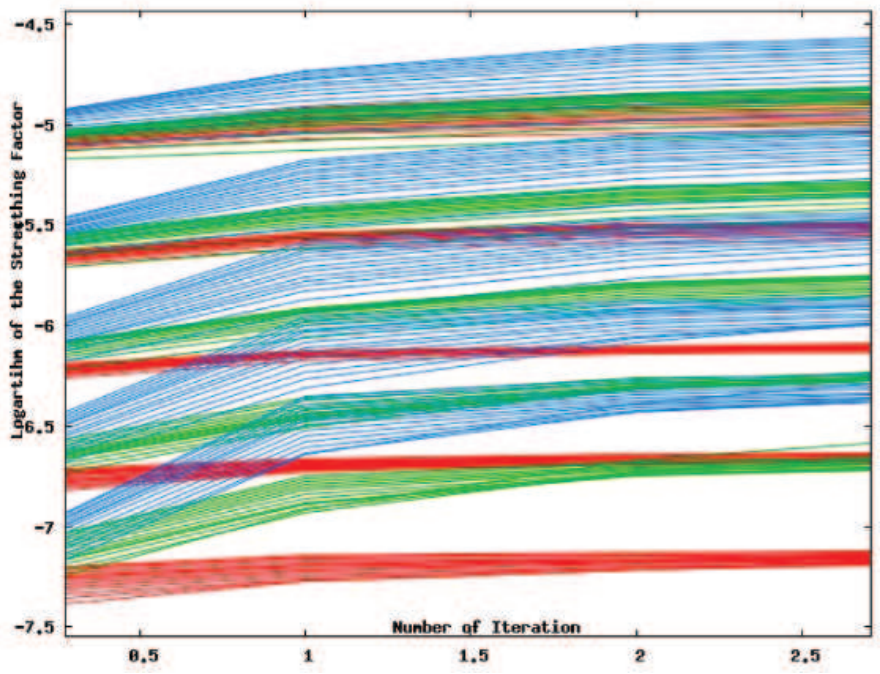

Figure 3.19. Lyapunov Exponents for relative humidities between 50 per cent - 70 per cent for PEG.

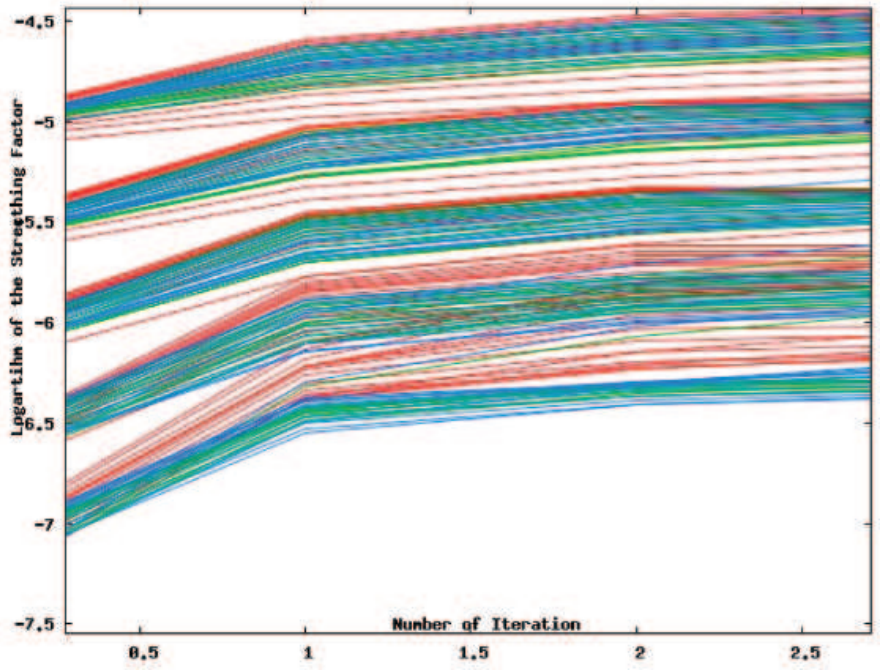

Figure 3.20. Lyapunov Exponents for relative humidities between 70 per cent - 80 per cent for PEG.

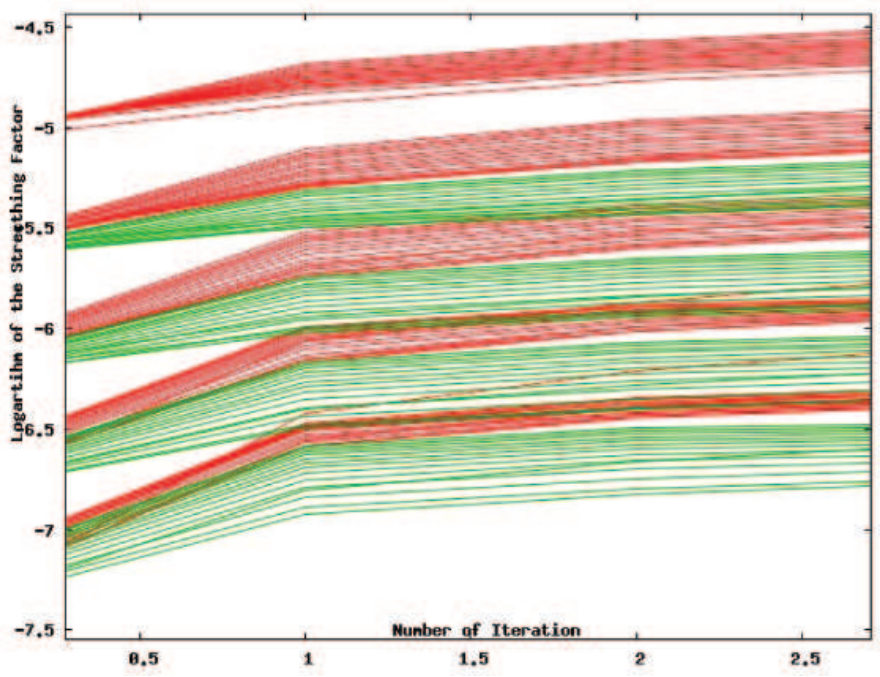

Figure 3.21. Lyapunov Exponents for relative humidities between 80 per cent - 90 per cent for PEG.

The irregular current characteristic under constant voltage for PEG-Si samples that we studied above gives instability problems and makes the material less suitable for a number of applications. To alleviate the instability problem of an irregular current characteristic under constant voltage in the PEG-Si samples at high relative humidity values, there are two methods; the first one is to enrich the PEG-Si samples with hydrogen, producing hydrogenated PEG-Si and the second one is to use hydrophobically modified PEG-Si samples, PAF-Si [19, 22, 24].

3.3. PAF - Si Analysis

After dissolving the modified PEG solution in doubly distilled water, the proper amount of Perfluoroalkylethylalcohol (PAF) solution is introduced to obtain PEG films including varying amounts of PAF. In this analysis, we are using two samples, one with 10 per cent and the other with 70 per cent PAF-Si. The transient current is shown below, in Figure 3.22. We start the analysis using the same procedure as we have done with PEG-Si, but we split the current data into equal relative humidity bins, denoted by vertical lines, vs time.

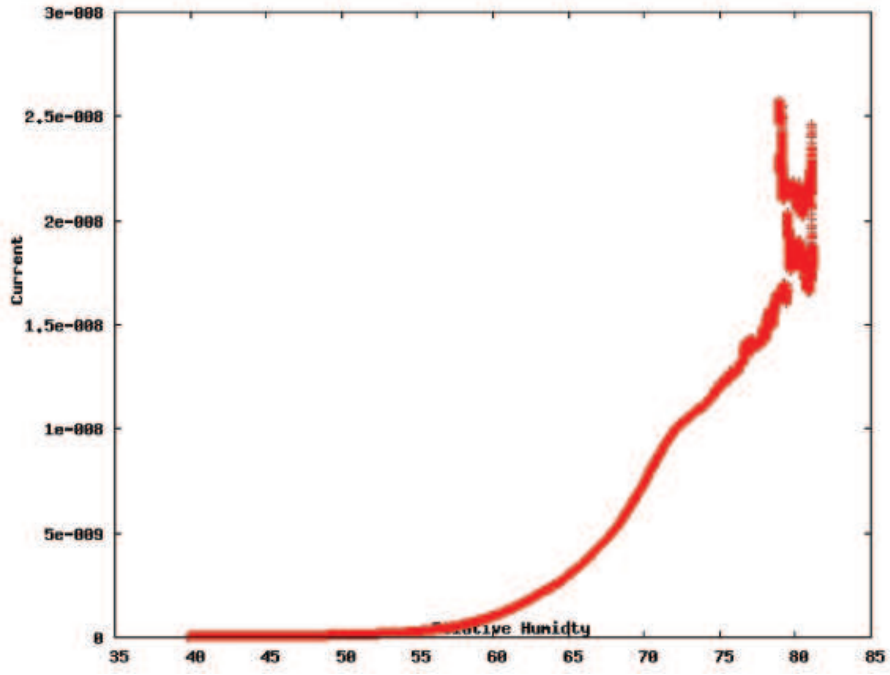

Figure 3.22. PAF Sample Current vs Relative Humidity.

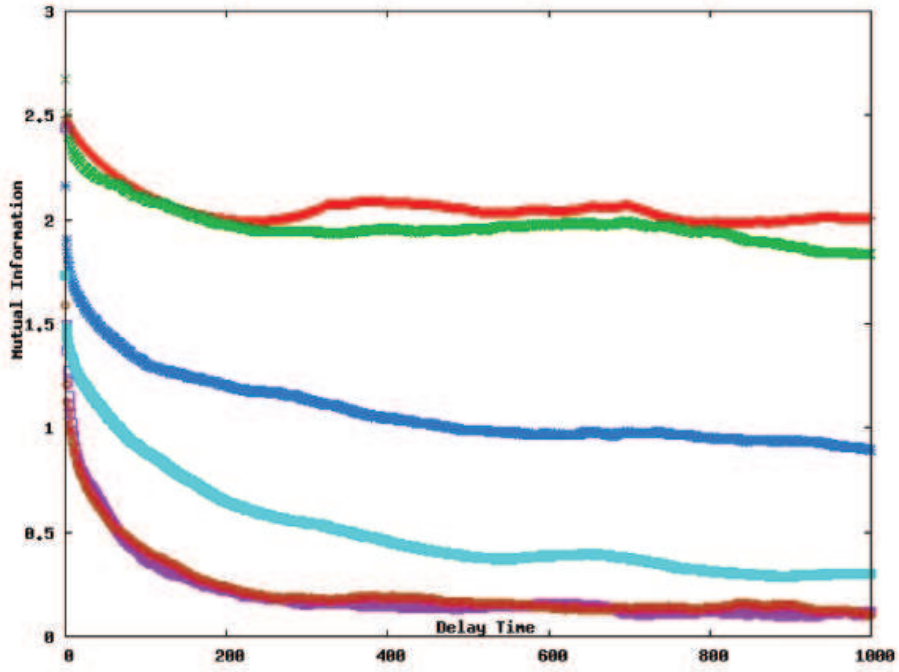

Figure 3.23. Mutual Information vs Delay Time for all split sets for PAF.

In the first step, as mentioned above, the mutual information vs delay time graph is drawn and the delay time is calculated as $t = 200$ seconds shown in Figure 3.23. The False Neighbors method gives us two different regions of the minimum embedding dimensions as shown in figures 3.24 and 3.25, each line shows a different relative hu-

midity region. For small humidity values, the embedding dimension behaves as if its minimum is at around 6 but for humidity values greater than 70 per cent our sample behaves like as a normal PEG-Si with embedding dimension, 12 [5, 6]. By using 10 per cent PAF, PEG-Si becomes more stable than pure PEG for relative humidities less then 70 per cent as shown in Figure 3.24. In Figure 3.25, the 70 per cent PAF sample is always more stable than both pure PEG and 10 per cent PAF; approximately all humidity values have small embedding dimensions around 5 or 6.

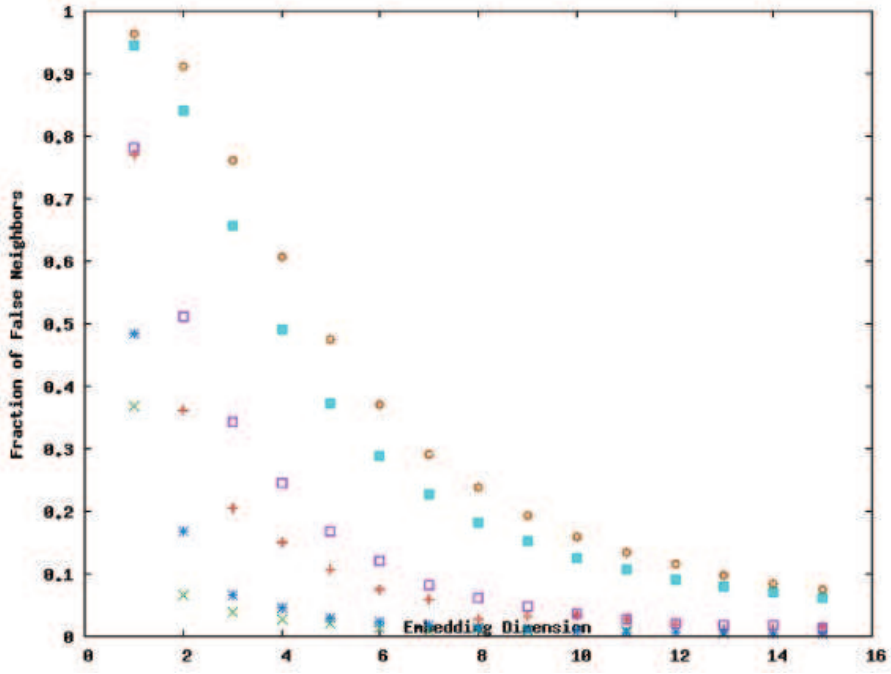

Figure 3.24. Embedding Dimension vs Fraction of False Neighbors for 10 per cent PAF Solution.

3.4. Hydrogenated PEG-Si Analysis

As mentioned in section 3.2, to alleviate the instability problem we can use hydrogenated pure PEG films. These modified thin films are obtained by heating the pure PEG film in a vacuum chamber that is filled with hydrogen gas until they are prepared. The transient current through a thin film of hydrogenated PEG is shown below, in Figure 3.26. We start the analysis using the same procedure as we have done with PEG-Si and PAF-Si, but we split the current data into equal relative humidity bins, denoted by vertical lines, vs time.

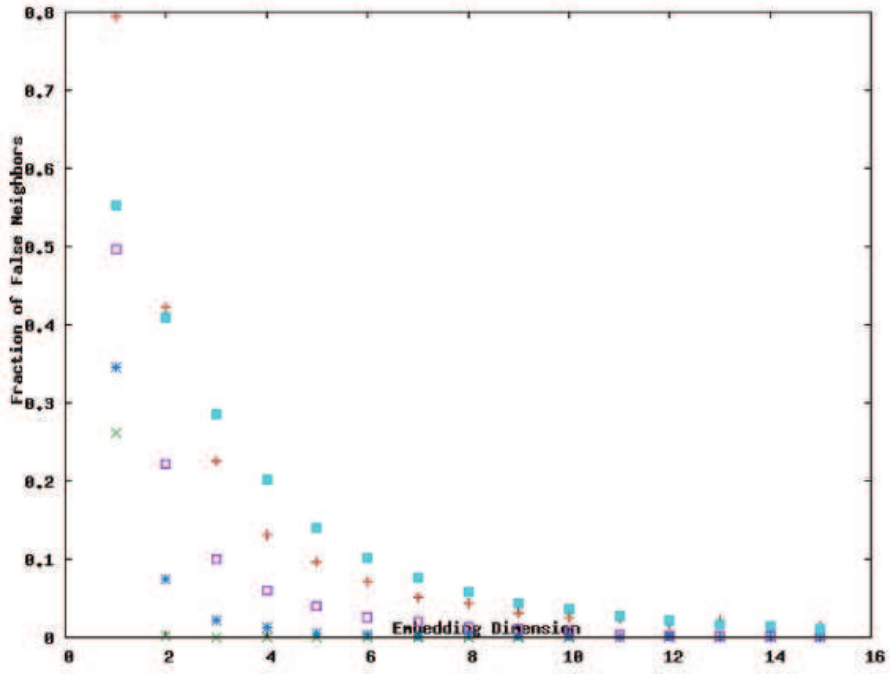

Figure 3.25. Embedding Dimension vs Fraction of False Neighbors for 70 per cent PAF Solution.

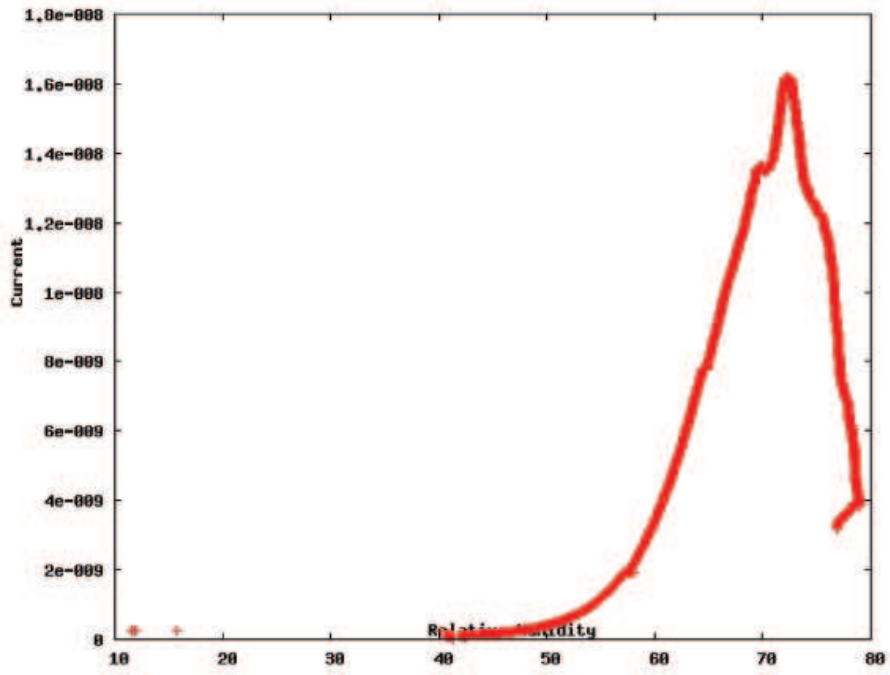

Figure 3.26. Hydrogenated PEG Sample Relative Humidity vs Current.

In the first step, as mentioned above, the mutual information vs delay time graph is drawn and the delay times are calculated as $t = 50$ s. for the 40 per cent - 50 per cent humidity range, $t = 100$ s. for the 50 per cent - 60 per cent humidity range and t =

200 seconds thereafter as shown in Figure 3.27. The False Neighbors method gives us two different regions of the minimum embedding dimensions as shown in Figure 3.28, each line shows a different relative humidity region.

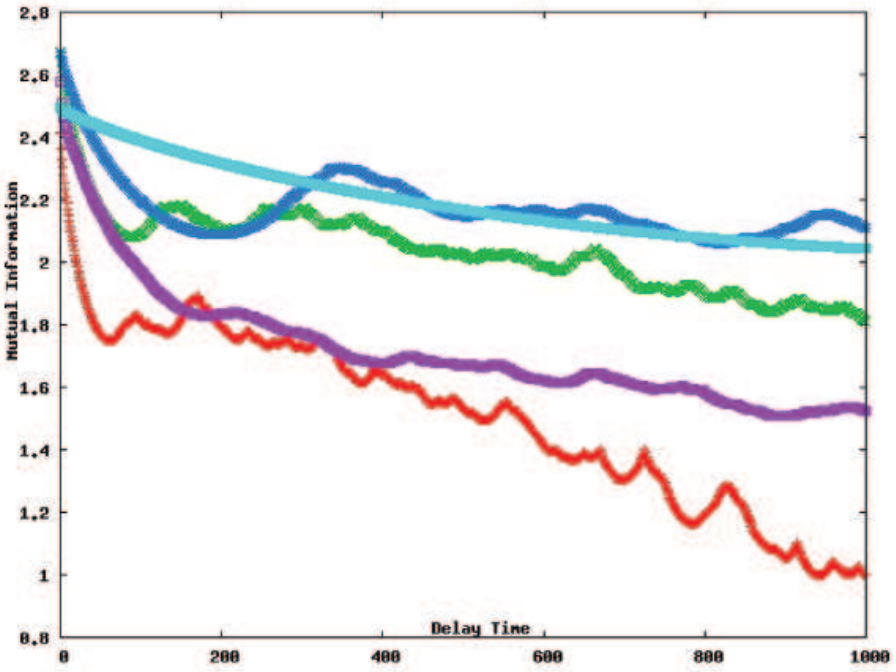

Figure 3.27. Mutual Information vs Delay Time for all split sets for Hydrogenated PEG.

For small humidity values, the embedding dimension behaves as if its minimum is at around 4 but for humidity values greater than 70 per cent our sample behaves like as a normal PEG-Si with embedding dimension, 12. By using hydrogenated PEG, we obtain a more stable material as evidenced by the significantly lower embedding than pure PEG and PAF for relative humidities less then 70 per cent as shown in figure 3.28.

A final point can be made here concerning the humidity dependence of the values of the embedding dimension and the Lyapunov exponent. Humidity based bins will be used. For pure PEG, the embedding dimension rests at 12 through the data, while the Lyapunov exponents range from 0.10 to 0.55. This is somewhat unusual since such a variation in Lyapunov exponent values would not be expected without a corresponding change in the embedding dimension. For PAF and hydrogenated PEG, Lyapunov

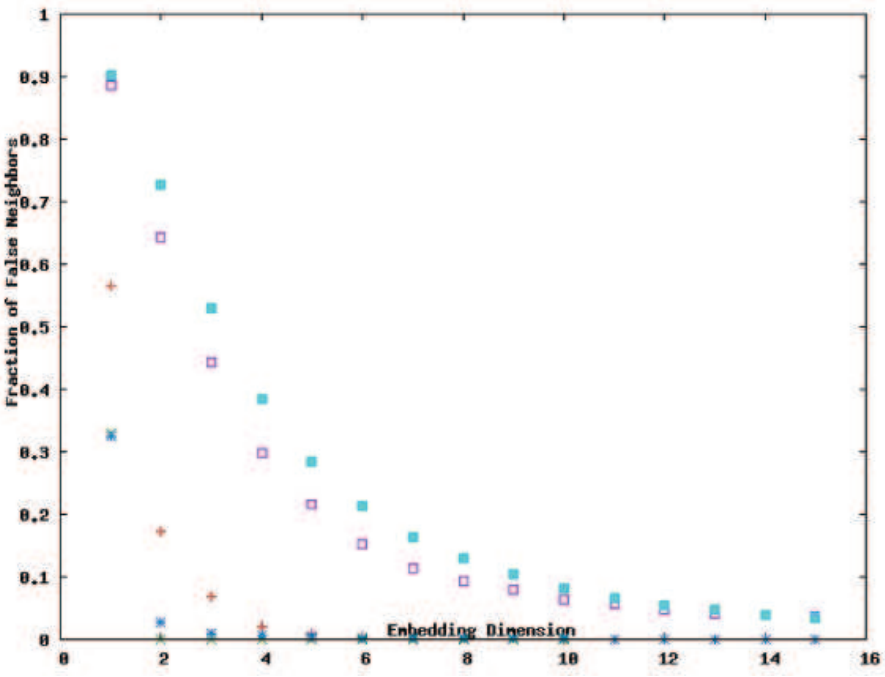

Figure 3.28. Embedding Dimension vs Fraction of False Neighbors for Hydrogenated PEG.

exponents range between 0.01 and 0.0001. These are much smaller values pointing to the more stable nature of these systems [20, 21, 22, 23].

4. DETRENDED FLUCTUATION ANALYSIS

4.1. Analysis of Time Series with DFA

Let us recall the fact that some fluctuation was observed in the values of the Lyapunov exponents as a function of relative humidity, including a slight decrease in the value of the maximal positive Lyapunov exponent after 80 per cent relative humidity. This would, at first sight, indicate agreement with the independent findings of [19] and serve to confirm the indication of an internal change (perhaps phase change) in the system. On the other hand, the rather large embedding dimension vis a vis an insufficient number of data points may make these changes stem from statistical fluctuations that might have affected convergence of the stretching algorithm. Noise known to be present in the data has also augmented the statistical fluctuation. Confirmation of these characterisics therefore requires a more detailed analysis of short and long range correlations as a function of relative humidity. To investigate this in more detail, we have applied the Detrended Fluctuation Analysis (DFA) method [25, 26, 27]. This is a scaling analysis method used to estimate long-range power-law correlation exponents. One integrates the time series of length N, then divides the result into boxes of equal length, n. In each box of length n, a least squares line is fit to the data. The y coordinate of the straight line segments is denoted by $y_{n(k)}$. Next, the integrated time series,$y_{(k)}$, is detrended by subtracting the local trend, $y_{n(k)}$, in each box. The root-mean-square fluctuation of this integrated and detrended time series is calculated as follows ;

$$F(n) = \sqrt{\frac{1}{N}\sum_{k=1}^{N}(y(k) - y_n(k))^2} \tag{4.1}$$

This computation is repeated over all time scales (box sizes) to characterize the relationship between $F(n)$, the average fluctuation, as a function of box size, n. A linear relationship on a log-log plot indicates the presence of power law scaling. Under such conditions, the fluctuations can be characterized by a scaling exponent, α, such that

$F(n)$: n^{α}. A crossover in the scaling exponent, α, indicates a transition from one type to a different type of underlying correlation, due to a transition in the dynamical properties.

4.2. PEG - Si DFA Analysis

As an initial attempt to confirm the suggestion of presence of short and long range correlations indicating changing regimes due to the different binding modes of the water molecules to the polymer, we used detrended fluctuation analysis on the whole data set. We observed two or three different regions where the slope is discontinuous; this points to changing dynamics of the correlations. One of the discontinuities is distinctly different since the slopes are 0.98, 1.03, and 1.8. Here the first and the second slopes can be assumed as approximately 1.0 therefore we can conclude the presence of two distinct regimes in Figure 4.1 [25, 26, 27].

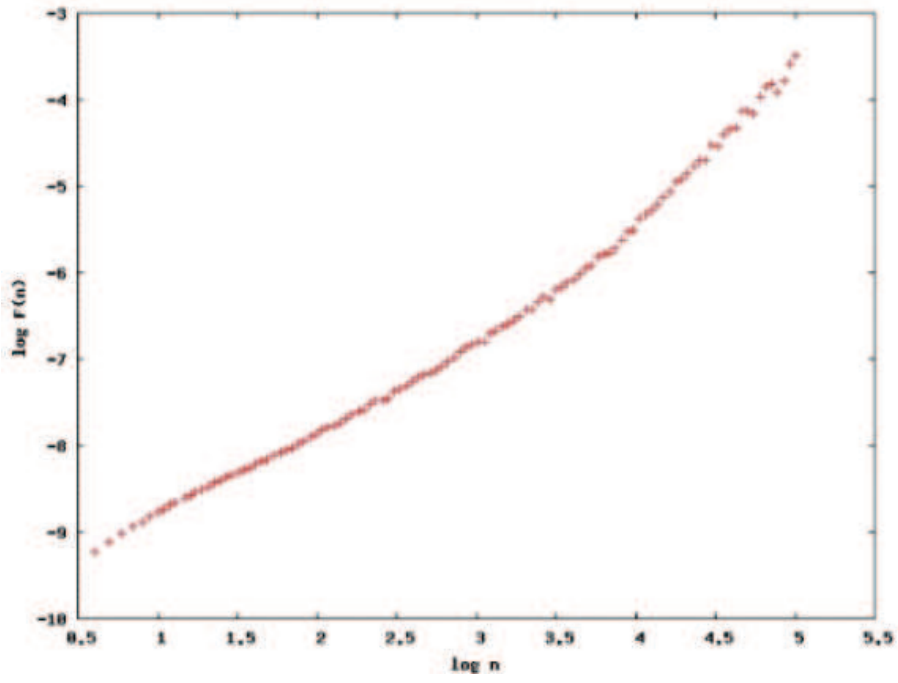

Figure 4.1. Two distinct regimes from the DFA - Pure PEG-Si graph.

4.3. PAF - Si DFA Analysis

For PAF-Si, we observed only one distinct region where the slope 1.8, is continuous; this points to an almost Brownian motion dynamics in the transport mechanism [16]. Here no change in the properties of the system(possible phase transition) can be said to occur in the system as shown in Figure 4.2 [25, 26, 27].

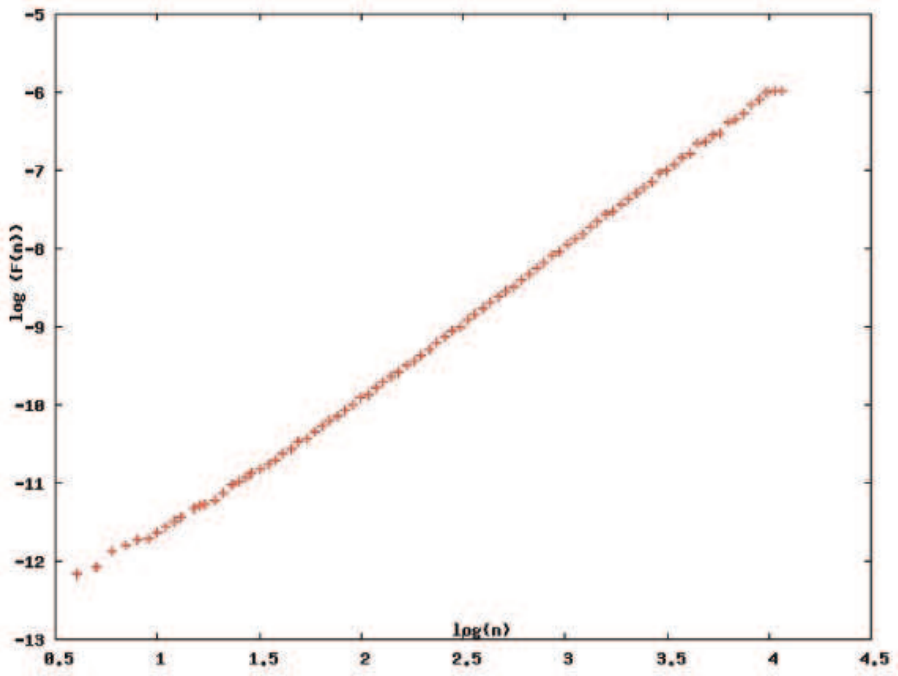

Figure 4.2. One regime from the DFA PAF-Si graph.

4.4. Hydrogenated PEG DFA Analysis

In order to study the effect of the binding modes of the water molecules to the polymer, we split the data into bins according to the relative humidity as in the Lyapunov exponent study. As shown in the Figure 4.3, for low relative humidities the scaling exponent is around 1.3 and there is no evidence for multiple regions; indicating brown fractal noise. As the relative humidity is increased, the presence of two regimes becomes more apparent; the scaling exponent of the short range correlation regime begins to decrease towards 1.0, while that of the long range correlation exponent persists at around 1.3 [25, 26, 27].

For Hydrogenated PEG, we also observed two different regions where the slope is discontinuous; this again points to two regimes involving changing dynamics of the correlations. The difference here is the relatively higher slopes in either region, namely 1.3 and 1.9. This indicates a drift towards Brown fractal and even Brownian motion [16].

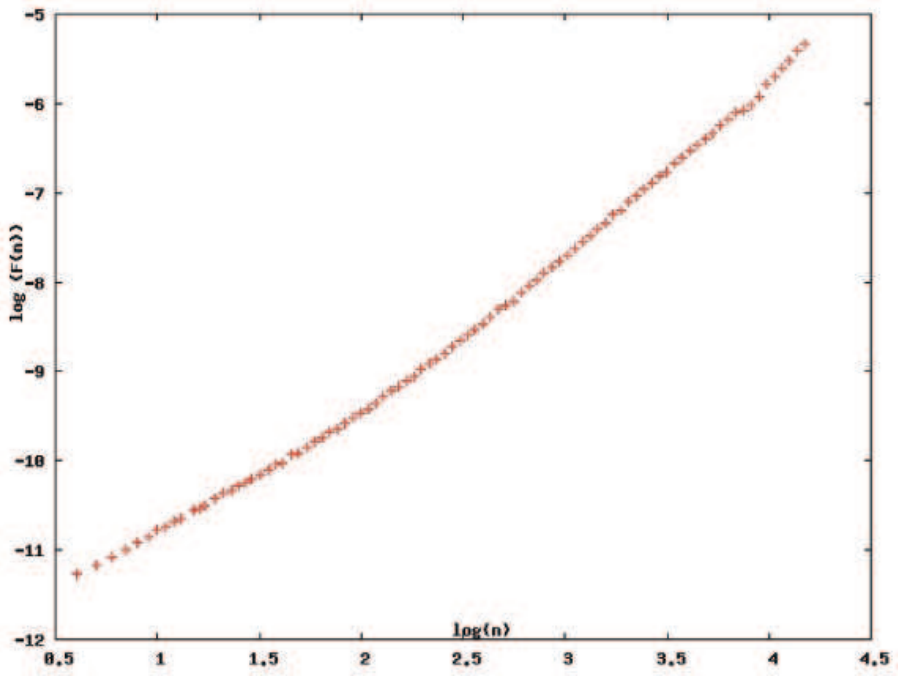

Figure 4.3. Two distinct regimes from the DFA - Hydrogenated PEG-Si graph.

5. CONCLUSIONS

To reach our objective of understanding the transient current behavior in a class of polymer thin films under changing humidity, the first step was to study the time behavior of the relative humidity for the pure PEG case, the PAF and Hydrogenated PEG cases. The time behavior of the relative humidity can be modelled by the absorption of the humidity introduced into the chamber by the sample. It is known that [11, 12, 13] many polymer molecules tend to absorb significant amounts of water when exposed to high humidity and the absorption can be modelled by a stretched exponential. We can conclude that the time behavior of the relative humidity can be modelled by the absorption of the humidity introduced into the chamber by the sample. Hence, any chaotic behavior that is identified is related to changes in the physical properties of the sample due to the absorption of humidity.

Having modelled the time behavior of the relative humidity, we investigated possible chaotic behavior of the pure PEG, PAF and Hydrogenated PEG case under varying humidity by binning the transient current data into time ranges and also into relative humidity ranges. We tried to make the best definitive determination concerning the humidity dependence of the values of the embedding dimension and possibly, the Lyapunov exponent. Using relative humidity based bins rather than time interval based bins improved our results and gave a better picture of the relative humidity dependence. For pure PEG, the embedding dimension rests at 12 through the data, while the Lyapunov exponents range from 0.10 to 0.55. This is somewhat unusual since such a variation in Lyapunov exponent values would not be expected without a corresponding change in the embedding dimension [11, 17, 22]. For PAF and hydrogenated PEG, Lyapunov exponents range between 0.01 and 0.0001, (may be compatible with zero because of systemmatic errors). These much smaller values point to the more stable nature of these latter systems.

Finally, by using DFA, we observed two or three different regions where the slope is discontinuous; this points to changing dynamics of the correlations. One of the

discontinuities is obviously distinct since the slopes are 0.98, 1.03, and 1.8. Here the first and the second slopes can be assumed as approximately 1.0 therefore we can conclude the presence of two distinct regimes for PEG-Si. For Hydrogenated PEG, we also observed two different regions where the slope is discontinuous; this again points to two regimes involving changing dynamics of the correlations. The difference here is the relatively higher slopes in either region, namely 1.3 and 1.9. This indicates a drift towards Brown fractal and even Brownian motion. For PAF-Si, we observed only one distinct region where the slope 1.8, is continuous; this points to an almost Brownian motion dynamics in the transport mechanism [16, 25, 26, 27]. Here no change in the properties of the system (such as phase transition) can be said to occur in the system.

REFERENCES

1. Taken, F., "Detecting strange attractors in turbulence", Lecture Notes in Mathematics, Vol. 898, pp. 366-381, 1981.

2. Sauer, T., J. Yorke and M. Casdagli, "Embedology", *Journal of Statistical Physics*, Vol. 65, pp. 579-616, 1991.

3. Grassberger, P., and I. Procaccia, "Measuring the strangeness of Strange Attractors", *Physica D*, Vol. 9, pp. 189-208, 1983.

4. Paladin, G. and A. Vulpani, "Anamolous scaling laws in multifractal objects", *Physics Reports*, Vol. 156, pp. 147-225, 1987.

5. Hegger, R., H. Kantz and T. Schreiber, "Practical implementation of nonlinear time series methods: The TISEAN package", *CHAOS*, Vol.94, pp.413-435, 1999.

6. Abarbanel, H.D.I., R. Brown, J. J. Sidorowich and L.S. Tsimring, "The analysis of observed chaotic data", *Reviews of Modern Physics*,Vol. 65, pp. 1331-1392, 1993.

7. Kantz, H., "A robust method to estimate the maximal Lyapunov exponent of a time series" *Physics Letters A*, Vol. 185, pp. 77-87, 1994.

8. Packard, N. H., J. P. Crutchfield, J. D. Farmer and R. S. Shaw, "Geometry from a time series", *Phys. Rev. Lett.*, Vol. 45,pp. 712, 1980.

9. Casdagli, M., S. Eubank, J. D. Farmer and J. Gibson, "State space reconstruction in the presence of noise", *Physica D*, Vol.51, pp. 52, 1991.

10. Martinerie, J. M., A. M. Albano, A. I. Mees and P. E. Rapp, "Mutual information, strange attractors, and the optimal estimation of dimension", *Phys. Rev. A*,Vol. 45, 7058, 1992.

11. Fatkullin, I., K. Kladko, I. Mitkov, A. R. Bishop, "Anomalous relaxation and self-organization in nonequilibrium processes" *Phys. Rev. E*, Vol. 63, 2001.

12. Bao, L. R., A. F. Yee, Charles Y., C. Lee, "Moisture absorption and hygrothermal aging in a bismaleimide resin", *Polymer Elsevier*, 2001.

13. Giaretto, V., G. Ruscica, E. Miraldi, "Stretched Exponential Relaxation Analysis Of The Moisture Diffusion in Carbon Fiber Samples" , *Modern Physics Letters B*, Vol. 8, pp. 965-975, 1994.

14. Buzug, T. and G. Pfister, "Optimal delay time and embedding dimension for delay-time coordinates by analysis of the global static and local dynamical behavior of strange attractors", *Phys. Rev. A*, Vol. 45, 1992.

15. Gibson, J. F., J. D. Farmer, M. Casdagli and S. Eubank, "An analytic approach to practical state space reconstruction", *Physica D*, Vol. 57, 1992.

16. Cecconi, F., M. Cencini, M. Falcioni and A. Vulpiani, "Brownian motion and diffusion: from stochastic processes to chaos and beyond", *Chaos*, Vol.15, 2005.

17. Eckmann, J. P., S. O. Kamphorst, D. Ruelle, "Ergodic Theory of Chaos and Strange Attractors", *Reviews of Modern Physics*, Vol. 57, pp. 617-656, 1985.

18. Schuster, H. G., "Deterministic Chaos", *WILEY-VCH*, Weinheim, 2005.

19. Erdamar, Ö, Y. Skarlatos, G. Aktaş and N. İnci, "Experimental investigation of the conduction mechanism of hydrogenated PEG thin films at high relative humidities", *Solid State Ionics*, Vol. 177, Issues 37-38, pp. 3217-3221, 2006.

20. Fraser, A. M. and H. L. Swinney, "Independent coordinates for strange attractors from mutual information", *Phys. Rev. A*, Vol. 33, 1986.

21. Grassberger, P., T. Schreiber and C. Schaffrath, "Non-linear time sequence Analysis", *Int. J. Bifurcation and Chaos*, pp.521, 1991.

22. Hacınlıyan, A., Y. Skarlatos, G.Sahin and G. Akın,"Signals of chaotic behavior in PMMA", *Chaos, Solitons and Fractals*, Vol.17, pp.575-585, 2003.

23. Hacınlıyan, A., Y. Skarlatos, H. A. Yıldırım and G. Sahin, "Characterization of Chaocity in The Transient Current Through PMMA Thin Films", *Physical Review B*, Vol. 73, Issue 13, 2006.

24. Da Silva R. L., R. M. Rubinger, A. G. De Oliveria and G. M. Riberio, "Nonlinear Dynamics Time Series Analysis of Chaotic Current Oscillations in a Semi-insulating GaAs Sample", *Braz. J. Phys.*, Vol. 32, Sao Paulo, 2002.

25. Hacınlıyan, A., Şahin, G., Erentürk, M., "Detrended fluctuation analysis in natural languages using non-corpus parametrization", *Chaos, Solitons and Fractals*, 2008.

26. Kantelhardt, J.W., E. Koscielny-Bunde, H.H.A. Rego, S. Havlin and A. Bunde, "Detecting long-range correlations with detrended fluctuation analysis", *Physica A*, Vol. 295, pp. 441, 2001.

27. Buldyrev, S. V., N. V. Dokholyan, A. V. Goldberger, S. Havlin, C. K. Peng and H.E. Stanley, "Analysis of DNA sequences using methods of statistical physics", *Physica A*, Vol. 249, pp. 430, 1998.